

Received July 31, 2015, accepted August 14, 2015, date of publication September 17, 2015, date of current version October 2, 2015.

Digital Object Identifier 10.1109/ACCESS.2015.2479406

# Energy and Spectrum Efficient Transmission Techniques Under QoS Constraints Toward Green Heterogeneous Networks

HARIS PERVAIZ, (Student Member, IEEE), LEILA MUSAVIAN, (Member, IEEE),  
QIANG NI, (Senior Member, IEEE), AND ZHIGUO DING, (Member, IEEE)

InfoLab21, School of Computing and Communications, Lancaster University, Lancaster LA1 4WA, U.K.

Corresponding author: H. Pervaiz (h.pervaiz@lancaster.ac.uk)

This work was supported in part by the U.K. Engineering and Physical Sciences Research Council under Grant EP/K011693/1 and in part by the European FP7 Programme under Grant PIRSES-GA-2013-610524.

**ABSTRACT** This paper proposes a joint energy efficiency (EE) and spectrum efficiency (SE) trade-off analysis as a multi-objective optimization problem (MOP) in the uplink of multi-user multi-carrier two-tier orthogonal frequency division multiplexing access heterogeneous networks subject to users' maximum transmission power and minimum rate constraints. The proposed MOP is modeled such that the network providers can dynamically tune the tradeoff parameters to switch between different communication scenarios with diverse design requirements. In order to find its Pareto optimal solution, the MOP is transformed, using a weighted sum method, into a single-objective optimization problem (SOP), which itself can further be transformed from a fractional form, by exploiting fractional programming, into a subtractive form. Since the formulated SOP is hard to solve due to the combinatorial channel allocation indicators, we reformulate the SOP into a better tractable problem by relaxing the combinatorial indicators using the idea of time-sharing. We then prove that this reformulated SOP is strictly quasi-concave with respect to the transmission power and the subcarrier allocation indicator. We then propose an iterative two-layer distributed framework to achieve an upper bound Pareto optimal solution of the original proposed MOP. The numerical simulations demonstrate the effectiveness of our proposed two-layer framework achieving an upper bound Pareto optimal solution, which is very close to an optimal solution, with fast convergence, lower and acceptable polynomial complexity, and balanced EE–SE tradeoff.

**INDEX TERMS** HetNets, green communications, energy efficiency and spectrum efficiency, resource allocation, small cells.

## I. INTRODUCTION

The heterogeneous networks (HetNets) include low-power overlaid base stations 'BSs' (or small cells, e.g., microcells, picocells, and femtocells) within the macrocell geographical area, deployed by either users or network operators who share the same spectrum with the macrocells [1]–[3]. The purpose of HetNets is to allow the user equipments (UEs) to access small cells, even though the UEs are within the coverage of macrocell [4]. HetNets aim at achieving high data rates with low powers while satisfying the users' quality-of-service constraints (in terms of minimum-rate requirements) by offloading the users with low signal-to-interference-plus-noise-ratios (SINR) from macrocells to the pico BSs. The deployment of small cells has a great potential to improve

the spatial reuse of radio resources and also to enhance the transmit power efficiency [5], and in turn, the energy efficiency (EE) of the network. EE is, in fact, one of the key performance indicators for the next generation wireless communications systems [6]. The motivation behind considering EE as the performance metric arises due to the current energy cost payable by operators for running their access networks as a significant factor of their operational expenditures (OPEX) [7]. It is however, known that most of EE gains are achieved with sacrifices in spectrum efficiency (SE) [8].

In this trend, the energy-efficient resource allocation technique is proposed in the uplink transmission scheme of traditional Orthogonal Frequency Division Multiple Access (OFDMA) systems [9]. This result is later generalized

to maximize the uplink EE in frequency selective channels in [10]. Similarly, a low complexity energy-efficient resource allocation in an uplink transmission scheme considering frequency-selective channels for multi-user networks, with and without fairness considerations, is studied in [11]. A energy-efficient resource allocation scheme for OFDMA systems under a fairness guarantee factor among users is proposed in [12], wherein, an optimisation problem is formulated as an integer fractional programming problem which is further simplified into an integer linear programming (ILP) form using an iterative fractional method. Further advances on green networking, which focus on the means to reduce the energy consumption in traditional wireless networks, can be accessed in [13] and [14]. Few of the recent works in the literature studying the characteristics of EE and SE analysis in traditional OFDMA systems is investigated for single user case in [15] and [16], and for multi user case in [17]–[19]. The impact of the number of deployed femtocells in a macrocell area, the average number of users, and the number of open channels in a femtocell using the Markov chain model on the EE and SE of two-tier femtocell networks is investigated in [20].

Most of the existing works in the literature for resource allocation in HetNets have focused on maximising either EE (in terms of Utopia EE for each individual user in [21] and [22], and in terms of the overall system EE in [22]–[24]) or SE [25]. In this trend, the EE-maximisation problem in an uplink of HetNets is analytically solved for a single user case under the minimum target rate and maximum transmission power constraints in [26]. Further, a distributed joint bandwidth and power allocation scheme to optimise EE for a set of users within the heterogeneous wireless networks is proposed in [27]. A joint BS association and power control scheme which is intent to satisfy the user's targeted SINR for the uplink of a large-scale HetNet is proposed in [28]. In [29], a distributed non-cooperative game was proposed to improve the system EE in the downlink transmission scheme of HetNets. The BSs autonomously choose their optimal transmission strategies while balancing the load among themselves and satisfying the users' quality-of-service (QoS) requirements [29]. A distributed novel cooperative game to establish cooperation among macrocell and femtocell to quantify the user's utility in terms of throughput and delay was formulated in [30]. Afterwards, a coalition formation algorithm was proposed to solve the formulated cooperative game so that it achieves a stable partition with the help of a recursive core [30].

We note that none of the previous works in the literature considered maximising overall system EE and SE of HetNets simultaneously, while imposing a threshold on the cross-tier interference to protect the macrocell user. Considering that simply maximising either EE or SE does not utilise the resources efficiently, there is an increasing attention in fifth generation (5G) networks to jointly optimise the two conflicting objectives, i.e., EE and SE. We note that the user lying within the coverage area of the heterogeneous environment

can efficiently utilise its transmission power for its allocated bandwidth in order to either improve its achievable EE or SE. One of the key performance indicators in the 5G networks is to reduce the EE-SE tradeoff region which can be enabled by HetNets.

According to the best of our knowledge, there is no work in the literature focusing on jointly optimising EE and SE in an uplink of multi-user two-tier HetNets considering the cross-tier interference limitations and providing users' QoS in terms of minimum rate requirements and maximum transmission power constraints. In this paper, we provide a formulation of an MOP framework for joint power allocation and subcarrier assignment for EE-SE tradeoff under maximum transmission power constraints when satisfying a rate QoS requirement in two-tier HetNets. The proposed multi-objective framework jointly performs power allocation and subcarrier assignment while optimising the two conflicting objectives, namely, EE and SE. We transform the formulated MOP into a single-objective optimisation problem (SOP) using a weighted sum method. Proving that the formulated SOP is strictly quasi-concave with respect to the transmit power, we derive a unique optimal solution. By exploiting the fractional programming concepts, the SOP problem can be transformed into an equivalent subtractive form which is tractable in nature. Then, an iterative two-layer solution combining Dinkelbach type method and Lagrangian dual decomposition approach is proposed to solve the formulated SOP.

The main contributions of this paper can be listed as:

- 1) We aim to jointly maximise the overall system EE and SE in an uplink of HetNets as an MOP by considering the cross-tier interference limitation, users' minimum QoS requirements and maximum transmission power constraint. Different from the existing works, which generally optimise the Utopia EE for each individual user [21], [22], or the system EE [22]–[24], our objective is to jointly maximise the overall system EE and SE considering the cross-tier interference threshold, users' minimum rate QoS requirements, and maximum transmission power constraints.
- 2) Different from the traditional EE or SE optimisation problems in HetNets, our aim is to formulate the uplink joint user association, subcarrier allocation and radio resource management problem in two-tier HetNets as a MOP jointly optimising conflicting objectives, maximising EE and SE. In order to find the Pareto-optimal solution, the MOP is transformed into a better tractable problem by using the weighted sum method exploiting the time sharing relaxation. We then prove that the transformed SOP is strictly quasi-concave.
- 3) We propose a distributed two-layer iterative framework to solve the SOP in its equivalent subtractive form by exploiting the fractional programming and Lagrangian Dual Decomposition (LDD) approach. The developed two-layer iterative framework can achieve the Pareto-optimal solution. The outer layer is solved using the Dinkelbach type method whereas the inner layer is

solved by dual decomposition. This process is repeated until both procedures converge to an optimal value.

- 4) The performance of our proposed distributed two-layer framework is evaluated by extensive simulations, which show that the proposed MOP approach outperforms the existing traditional approaches, such as maximising EE subject to an SE constraint or maximising SE subject to an EE constraint in terms of flexibility and scalability to dynamically tune the tradeoff among different solutions depending on the practical goals and requirements of the operators. The proposed framework with polynomial complexity can achieve the performance very close to an optimal solution achieved by exhaustive search with an exponential complexity.

The remainder of the paper is organised as follows. In Section II, we describe the system model and define the concept of EE and SE. In Section III, we formulate the problem of jointly optimising EE and SE in an uplink of two-tier HetNets as an MOP. In Section IV, a two-layer solution is proposed to obtain the optimal allocation strategy to solve the formulated MOP. Numerical results are presented to demonstrate the effectiveness of the proposed approach in Section V. Section VI concludes the paper.

## II. SYSTEM MODEL

We consider an uplink two-tier HetNets consisting of  $M$  networks (i.e., one macrocell ( $m_0$ ), overlaid with  $M - 1$  pico BSs ( $m_1, \dots, m_{M-1}$ )), with a total number of users  $N$  and a total number of subcarriers  $K$ . We assume that the  $M - 1$  pico BSs are deployed around the edge of the reference macrocell  $m_0$ . Let define the index set of all subcarriers as  $\mathcal{K} = \{1, \dots, K\}$ , the set of all users as  $\mathcal{N} = \{1, \dots, N\}$  and the set of all networks as  $\mathcal{M} = \{m_0, m_1, \dots, m_{M-1}\}$ . The total number of available networks in two-tier HetNets can be calculated as follows [31]:

$$M = 1 + \beta \left( \frac{(R_{m_0} + R_i)^2 - (R_{m_0} - R_i)^2}{R_i^2} \right), \quad (1)$$

where  $R_{m_0}$  and  $R_i$  represent the radius of macrocell and pico BS, respectively. When  $\beta = 0$ , it is the case of macrocell only, and therefore,  $M = 1$ , whereas in the case of HetNets,  $0 < \beta \leq 1$  which indicates the number of pico BSs per macrocell.

Each network  $m \in \mathcal{M}$  has its own bandwidth  $B_m$  equally divided among its subcarriers<sup>1</sup>  $\mathcal{K}_m$ , where  $\mathcal{K}_m = \{1, \dots, K_m\}$  represent the set of subcarriers in network  $m$ . The pico BS is connected to the macrocell via a high capacity wired backhaul. We further assume that the channel state information (CSI) corresponding to each subcarrier is perfectly known to the UE transmitters.

<sup>1</sup>It is worth to mention that the partition of subcarriers into the sets  $\mathcal{K}_{m_0}$  and  $\mathcal{K}_{m_i}$ ,  $i = 1, 2, \dots, M - 1$  is not predefined in the present formulation. The optimisation problem in (13a)-(13f) include an optimisation over  $\mathcal{K}_{m_0}$  and  $\mathcal{K}_{m_i}$ ,  $i = 1, 2, \dots, M - 1$  as well.

To maintain the QoS requirements, each user has a minimum-rate requirement constraint. We assume that the required minimum-rate level of all users are identical and is equal to  $R_{\min}$ . Assume  $\sigma_{k,n}^{(m_0)}$  and  $\sigma_{k,n}^{(m_i)}$  denoting the subcarrier allocation indices for macrocell  $m_0$  and pico BS  $m_i$ , respectively. Particularly, when subcarrier  $k \in \mathcal{K}_{m_i}$  is allocated to user  $n$ , then  $\sigma_{k,n}^{(m_i)} = 1$ , and otherwise,  $\sigma_{k,n}^{(m_i)} = 0$ . Similarly, if the subcarrier  $k \in \mathcal{K}_{m_0}$  is allocated to user  $n$ ,  $\sigma_{k,n}^{(m_0)} = 1$ , and otherwise,  $\sigma_{k,n}^{(m_0)} = 0$ . The instantaneous data rate achieved on each subcarrier  $k$  by user  $n$  for macrocell  $m_0$  and pico BS  $m_i$  can be written as follows:

$$r_{k,n}^{(m_0)} = \sigma_{k,n}^{(m_0)} B_k \log_2 \left( 1 + \gamma_{k,n}^{(m_0)} \times p_{k,n}^{(m_0)} \right) \quad (2a)$$

$$r_{k,n}^{(m_i)} = \sigma_{k,n}^{(m_i)} B_k \log_2 \left( 1 + \gamma_{k,n}^{(m_i)} \times p_{k,n}^{(m_i)} \right), \quad \forall i \in \{1, 2, \dots, M - 1\} \quad (2b)$$

where  $B_k$  is the subcarrier bandwidth spacing assumed to be fixed in different networks. Here,  $p_{k,n}^{(m_i)}$  and  $p_{k,n}^{(m_0)}$  indicate the power allocated to the subcarrier  $k$  for user  $n$  in the pico BS  $m_i$  and macrocell  $m_0$ , respectively. Similarly, the rate of user  $n$  using subcarrier  $k$  choosing macrocell or pico BS  $m_i$  is represented by  $r_{k,n}^{(m_0)}$  and  $r_{k,n}^{(m_i)}$ , respectively.  $\gamma_{k,n}^{(m_0)}$  and  $\gamma_{k,n}^{(m_i)}$  represent the channel-to-noise-ratio (CNR) of user  $n$  on subcarrier  $k$  in the macrocell  $m_0$  and pico BS  $m_i$ , respectively, and are defined as follows:

$$\gamma_{k,n}^{(m_0)} = \frac{|h_{k,n}^{(m_0)}|^2}{\left( B_k N_0 + \sum_{\substack{m \in \mathcal{M} \\ m \neq m_0}} \sum_{n \in \mathcal{N}_m} \sigma_{k,n}^{(m)} p_{k,n}^{(m)} g_{k,n}^{mm_0} \right) \text{PL}_n^{(m_0)}}, \quad (3a)$$

$$\gamma_{k,n}^{(m_i)} = \frac{|h_{k,n}^{(m_i)}|^2}{\left( B_k N_0 + \sum_{n \in \mathcal{N}_{m_0}} \sigma_{k,n}^{(m_0)} p_{k,n}^{(m_0)} g_{k,n}^{m_0 m_i} \right) \text{PL}_n^{(m_i)}}, \quad \forall i \in \{1, 2, \dots, M - 1\} \quad (3b)$$

where  $h_{k,n}^{(m_0)}$  and  $h_{k,n}^{(m_i)}$  represent the channel amplitude gains for user  $n$  on subcarrier  $k$  from macrocell  $m_0$  and pico BS  $m_i$ , respectively.  $\mathcal{N}_m$  and  $\mathcal{N}_{m_0}$  represent the set of users associated with network  $m$  and macrocell  $m_0$ , respectively. The distance-based path loss in macrocell  $m_0$  and pico BS  $m_i$  are denoted by  $\text{PL}_n^{(m_0)}$  and  $\text{PL}_n^{(m_i)}$ , respectively. Note that in (3a) and (3b), the co-tier interference from other pico BSs or macrocells is assumed to be a part of thermal noise  $N_0$  due to the severe penetration loss and low transmission power of pico BSs as mentioned in [25] and [32].

The focus of this work is to investigate the trend of EE-SE tradeoff in the two-tier HetNets consisting of a macrocell  $m_0$  overlaid with a number of pico BSs  $m_i$ ,  $\forall i \in \{1, 2, \dots, M - 1\}$ , the co-tier interference caused from the neighbouring macrocells or pico BSs can be easily considered and will appear as a constant term in (3a) and (3b).

In order to protect the macrocell users QoS, we implement the cross-tier interference protection by imposing the

maximum cross-tier interference threshold suffered by macro BS. Let  $I_k^{\text{th}}$  denote the maximum threshold interference level on subcarrier  $k$  for the macro BS, we have,

$$\sum_{\substack{m \in \mathcal{M} \\ m \neq m_0}} \sum_{n \in \mathcal{N}_m} \tilde{\sigma}_{k,n}^{(m)} p_{k,n_m^*}^{(m)} g_{k,n_m^*}^{(m)} \leq I_k^{\text{th}}, \quad \forall k, \quad (4)$$

where  $n_m^* = \arg \max_n g_{k,n}^{(m)}, \forall n \in \mathcal{N}_m$  using the concept of the reference user [33]. The aggregate rate for the  $n^{\text{th}}$  user in macrocell  $m_0$  and pico BS  $m_i$  are shown as follows:

$$r_n^{(m_0)} = \sum_{k \in \mathcal{K}_{m_0}} r_{k,n}^{(m_0)}, \quad \forall n \in \mathcal{N} \quad (5a)$$

$$r_n^{(m_i)} = \sum_{k \in \mathcal{K}_{m_i}} r_{k,n}^{(m_i)}, \quad \forall n \in \mathcal{N}, \quad \forall i \in \{1, 2, \dots, M-1\} \quad (5b)$$

The overall rate of HetNets,  $R$  is composed of two components; The first component is the sum rate of the users choosing macrocell and the second one is the sum rate of the users choosing pico BS, formulated as

$$R = \sum_{n \in \mathcal{N}_{m_0}} r_n^{(m_0)} + \sum_{i=1}^{M-1} \left( \sum_{n \in \mathcal{N}_{m_i}} r_n^{(m_i)} \right), \quad (6)$$

where  $\mathcal{N}_{m_0}$  and  $\mathcal{N}_{m_i}$  denote the set of users associated with macrocell  $m_0$  and pico BS  $m_i$ , respectively.

In order to avoid frequent vertical handoffs in HetNets, user association rules are defined for wireless transmissions [2]. In traditional homogeneous cellular networks, the user association is based on the received signal strength. Unique association of users with the macrocell or pico BS is assumed [2]. Therefore, a feasible subcarrier assignment index matrix  $C_m$  is given by:

$$C_m \in \mathcal{C}_m = \left\{ \left( \sigma_{k,n}^{(m)} \right)_{k=1, n=1}^{K, N_m} \left| \sum_{n \in \mathcal{N}} \sigma_{k,n}^{(m)} \leq 1, \quad \forall k \in \mathcal{K}_m; \right. \right. \\ \left. \left. \sigma_{k,n}^{(m)} \in \{0, 1\}, \quad \forall n \in \mathcal{N}_m, \quad \forall k \in \mathcal{K}_m \right\}, \quad (7)$$

For simplicity, we assume that a set of available networks in two-tier HetNets are known. In practice, the transmission power available at user  $n$  is limited to a maximum threshold, i.e.,  $P_n^{\text{max}}$ , which can be formulated as:

$$P_n \leq P_n^{\text{max}}, \quad \forall n \in \{1, 2, \dots, N\} \quad (8a)$$

$$P_n = \sum_{k \in \mathcal{K}_m} p_{k,n}^{(m)}, \quad \forall m \in \{m_0, m_1, m_2, \dots, m_{M-1}\} \quad (8b)$$

In an uplink transmission scenario, multiple users transmit data towards a BS so each communication link between user and BS introduces an individual circuit power [9]. Since the circuit power is related to the UE handsets, the circuit power in macrocell and pico BSs are denoted by  $P_C^{(m_0)}$  and  $P_C^{(m_i)}$ , respectively such that  $P_C^{(m_0)} = P_C^{(m_i)} = P_C$ . Hence, the overall power consumption in an uplink of HetNets is modelled as:

$$P = \epsilon_0 P_T + N \times P_C, \quad (9a)$$

$$P_T = \sum_{m \in \mathcal{M}} \sum_{k \in \mathcal{K}_m} \sum_{n \in \mathcal{N}} \sigma_{k,n}^{(m)} p_{k,n}^{(m)}, \quad (9b)$$

where  $\epsilon_0$  is the inverse of power amplifier efficiency.

The EE ( $\eta_{EE}$ ) is defined as the amount of data transferred per unit energy consumed by the system (usually measured in (b/J) and is given by:

$$\eta_{EE} = \frac{R}{P} = \frac{\sum_{m \in \mathcal{M}} \sum_{k \in \mathcal{K}_m} \sum_{n \in \mathcal{N}} r_{k,n}^{(m)}}{\epsilon_0 \left( \sum_{m \in \mathcal{M}} \sum_{k \in \mathcal{K}_m} \sum_{n \in \mathcal{N}} \sigma_{k,n}^{(m)} p_{k,n}^{(m)} \right) + N \times P_C} \quad [\text{bits/Joule}], \quad (10)$$

In (10),  $r_{k,n}^{(m)}$  is concave with respect to the transmission power  $P_T$  because  $P_T$  is a non decreasing linear function of  $p_{k,n}^{(m)}$ . Since, the  $\eta_{EE}$  is strictly quasi-concave with respect to transmission power  $P_T$ , there exists one and only one optimal solution that maximises  $\eta_{EE}$ , denoted by  $P_{\eta_{EE}}^*$ .  $\eta_{EE}$  strictly increases with  $P_T \in [0, P_{\eta_{EE}}^*]$  while it strictly decreases with  $P_T \in [P_{\eta_{EE}}^*, \infty)$ . SE ( $\eta_{SE}$ ), on the other hand, is a measure that reflects the efficient utilization of the available spectrum in terms of throughput and is commonly defined as the amount of throughput that the BS can transmit over a given bandwidth, expressed in b/s/Hz.  $\eta_{SE}$  is a strictly increasing function of transmission power  $P_T$ , and is concave with  $P_T$ . The SE ( $\eta_{SE}$ ) is defined as:

$$\eta_{SE} = \frac{\sum_{m \in \mathcal{M}} \sum_{k \in \mathcal{K}_m} \sum_{n \in \mathcal{N}} r_{k,n}^{(m)}}{B} \\ = \frac{\sum_{m \in \mathcal{M}} \sum_{k \in \mathcal{K}_m} \sum_{n \in \mathcal{N}} r_{k,n}^{(m)}}{\sum_{k \in \mathcal{K}} B_k} \quad [\text{bits/s/Hz}], \quad (11)$$

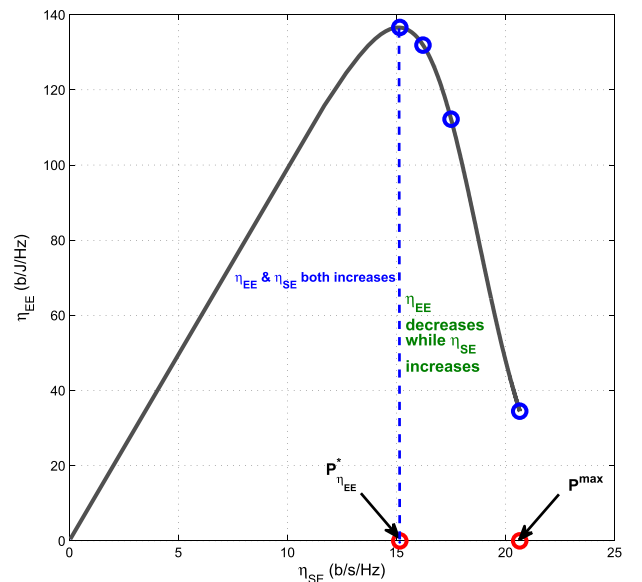


FIGURE 1.  $\eta_{EE}$ - $\eta_{SE}$  tradeoff curve as a function of transmission power  $P_T$ .

First of all, in order to give readers an intuitive insight into our problem to jointly optimise EE and SE, Fig. 1 shows

achievable EE and SE as a function of transmission power  $P_T$  with  $N = 10$ ,  $K = 10$ ,  $B_k = 30$  kHz,  $P_C = 0.1$  W and  $P_{\max} = 0.5$  W based on (10) and (11), respectively. From Fig. 1, it is quite obvious that in most of the cases, it is not usually possible to optimise both EE and SE simultaneously. In details, EE and SE both increase with transmission power  $P_T$  until the energy-efficient transmission power  $P_T = P_{\eta_{EE}}^*$ . However, when  $P_T > P_{\eta_{EE}}^*$  and afterwards, EE decreases with an increase in SE as shown in Fig. 1. The corresponding optimal transmit power (highlighted by red circles in Fig. 1) to maximise EE and SE individually without any QoS requirements are obtained by solving (10) and (11) using standard convex optimisation methods. To visualise the effect of QoS requirements on the optimisation of EE and SE, Fig. 1 depicts the corresponding optimal transmit power which maximises EE and SE individually with the QoS requirement set at 15, 16, 18 and 20 b/s/Hz as indicated by series of blue circles. It is quite obvious that a particular QoS requirement constraint can effect the existence of power region which allows all the constraints to be met simultaneously. Secondly, due to the Shannon Hartley theorem, increasing the transmit bandwidth reduces the transmit power for a same target rate requirement. For achieving a fixed minimum rate, as the bandwidth increases, EE increases whereas SE decreases. Finally, the maximisation of EE produces a different optimal point if the user can access subcarriers with better channel gains resulting in improving its utility. This motivates us to dynamically tune the EE and SE trade-off curve dependent on the available resources, in terms of bandwidth and the transmission power for next generation networks to achieve two-fold benefits in the form of satisfactory SE and saving as much transmission power as possible. It is also worthwhile to mention that in most of the power regions, the power allocation strategies to increase these metrics are conflicting approaches. This motivates the work in the following section which is to jointly optimise EE and SE using a multi-objective optimisation problem.

### III. PROBLEM FORMULATION OF EE-SE TRADEOFF

Our goal is to optimise EE and SE simultaneously. We start by formulating the joint EE and SE trade-off with the minimum throughput and maximum transmission power constraints in an uplink transmission scheme of Two-Tier HetNets as a multi-objective optimisation approach. The MOP can be formulated as follows:

$$\max_{\sigma_{k,n}^{(m)}, p_{k,n}^{(m)}} \eta_{EE} \text{ and } \max_{\sigma_{k,n}^{(m)}, p_{k,n}^{(m)}} \eta_{SE} \quad (12)$$

To solve this MOP, we utilise the concept of Pareto optimality [34]. The EE-SE tradeoff is usually illustrated as a two dimensional curve consisting of set of all feasible  $(\eta_{SE}, \eta_{EE})$  pairs.

*Definition 1:* A point  $p_0 \in \mathcal{P}_S$ , where  $\mathcal{P}_S = \{P_T | P_{\min} \leq P_T \leq P_n^{\max}\}$  is Pareto efficient if and only if there does not exist any other point  $p_1 \in \mathcal{P}_S$  such that  $\eta_{EE}(p_1) \geq \eta_{EE}(p_0)$ ,  $\eta_{SE}(p_1) \geq \eta_{SE}(p_0)$  and at least one  $\eta_{EE}$  or  $\eta_{SE}$  has been

strictly improved. In simple terms, a point is Pareto efficient if there is no other point that can improve both  $\eta_{EE}$  and  $\eta_{SE}$  simultaneously. The set of all Pareto efficient points is called the Pareto Frontier or the complete Pareto optimal set. The Pareto Frontier illustrates an optimal tradeoff between  $\eta_{SE}$  and  $\eta_{EE}$  such that it provides the maximum value of  $\eta_{SE}$  ( $\eta_{EE}$ ) for a given  $\eta_{EE}$  ( $\eta_{SE}$ ). In particular, the weighted sum method can provide the complete Pareto optimal set of the considered problem by solving the MOP and provide the necessary condition for Pareto optimality.

In MOP, the process of ordering the objectives can be done either as priori or posteriori of executing the optimisation algorithm. We combine the maximisation of EE and SE by choosing appropriate weights decided a priori. Since the bandwidth is larger than the transmission power so a simple summation of EE and SE will tend to focus on the optimisation of EE. In order to maintain the balance between EE and SE, we transform the optimisation problem using the normalised factors  $\theta_{EE}$  and  $\theta_{SE}$  such that EE and SE are in the similar scale. Using the weighted sum method [35], we can convert the MOP in (12) into SOP defined as:

$$\max_{\sigma_{k,n}^{(m)}, p_{k,n}^{(m)}} \omega \theta_{EE} \eta_{EE} + (1 - \omega) \theta_{SE} \eta_{SE} \quad (13a)$$

$$\text{s.t. } \sum_{m \in \mathcal{M}} \sum_{k \in \mathcal{K}_m} r_{k,n}^{(m)} \geq R_n^{\min}, \quad \forall n. \quad (13b)$$

$$\sum_{m \in \mathcal{M}} \sum_{k \in \mathcal{K}_m} \sigma_{k,n}^{(m)} p_{k,n}^{(m)} \leq P_n^{\max}, \quad \forall n. \quad (13c)$$

$$\sum_{\substack{m \in \mathcal{M} \\ m \neq m_0}} \sum_{n \in \mathcal{N}_m} \tilde{\sigma}_{k,n}^{(m)} p_{k,n}^{(m)} g_{k,n}^{mm_0} \leq I_k^{\text{th}}, \quad \forall k. \quad (13d)$$

$$\sum_{n \in \mathcal{N}_m} \sigma_{k,n}^{(m)} \leq 1, \quad \forall k, \forall m. \quad (13e)$$

$$p_{k,n}^{(m)} \geq 0, \quad \sigma_{k,n}^{(m)} \in \{0, 1\}, \quad \forall n, \forall k, \forall m. \quad (13f)$$

Here, (13a) represents the EE-SE tradeoff optimisation problem and  $\omega$  is the tradeoff parameter such that  $0 \leq \omega \leq 1$  which provides flexibility to achieve the EE-SE tradeoff. The QoS constraint (13b) guarantees the minimum user rate requirement. Constraint (13c) limits the maximum transmission of each user to be less than  $P_n^{\max}$ . The constraint in (13d) sets the maximum tolerable cross-tier interference on each subcarrier  $k$  of the macrocell  $m_0$ . The constraint (13e) and (13f) ensure that each subcarrier can be only assigned to at most one user in each network  $m$  at a time. The constraint (13f) also confirms the feasibility of non-negative transmission power on each subcarrier. It should be noted that when  $p_{k,n}^{(m)*} \geq P_n^{\max}$ , the proposed solution for (13a) contains a unique global optimal solution, i.e.,  $P_n^{\max}$ . Therefore, we will analyse the case of  $p_{k,n}^{(m)*} < P_n^{\max}$  for the rest of this paper. Hence, (13a) can be written as

$$\bar{\eta} = \max_{\sigma_{k,n}^{(m)}, p_{k,n}^{(m)}} \theta_{EE} \eta_{EE} + \left( \frac{1 - \omega}{\omega} \right) \theta_{SE} \eta_{SE} \quad [\text{bits/s}] \quad (14)$$

In (14), we can replace  $\left(\frac{1-\omega}{\omega}\right)$  with  $\alpha$  which can hold any real value from zero to  $\infty$ . After some mathematical manipulations, (14) can be simplified to

$$\eta = \frac{\bar{\eta}}{\theta_{EE}} = \max_{\sigma_{k,n}^{(m)}, p_{k,n}^{(m)}} \eta_{EE} + \alpha \left( \frac{\theta_{SE} \eta_{SE}}{\theta_{EE}} \right) \quad [\text{bits/Joule}], \quad (15a)$$

$$\text{s.t. (13b) - (13e).} \quad (15b)$$

$$\alpha \geq 0, \quad p_{k,n}^{(m)} \geq 0, \quad \tilde{\sigma}_{k,n}^{(m)} \in \{0, 1\}, \quad (15c)$$

$$\forall n, \forall k, \forall m.$$

where  $\alpha \in [0, \infty)$  is the weighted coefficient. When  $\alpha = 0$ , the problem in (15a) is transformed into an EE maximisation problem whereas it is transformed into an SE maximisation problem when  $\alpha \rightarrow \infty$ . In other words, the importance of SE gradually increases as  $\alpha$  increases from 0 to  $\infty$ .

*Remark 1:* The optimisation problem in (15a) has two important properties stated as follow:

*Property 1:* The optimal transmit power to achieve  $\eta^*$  is non-decreasing with the weighted coefficient  $\alpha$ . When  $\alpha = 0$ , the optimal transmit power is  $P_{\eta_{EE}}^*$ ; whereas when  $0 < \alpha < \infty$ , the optimal transmit power strictly increases with  $\alpha$  until it approaches the maximum transmit power. In other words, an increase of  $\alpha$  gives more importance to  $\eta_{SE}$  resulting in lesser importance to  $\eta_{EE}$ . Due to this, the optimal transmit power shift from  $P_{\eta_{EE}}^*$  towards the maximum transmit power.

*Property 2:*  $\eta_{SE}$  is non-decreasing with the weighted coefficient  $\alpha$ , while  $\eta_{EE}$  is non-increasing with the weighted coefficient  $\alpha$ . Lets us assume that  $\alpha_1$  and  $\alpha_2$  are the weighted coefficients such that  $\alpha_2 > \alpha_1$ . From property 1, the optimal transmit power  $P_{\eta_{\alpha_2}}^* > P_{\eta_{\alpha_1}}^*$ . As  $\eta_{SE}$  increases monotonically with transmit power whereas  $\eta_{EE}$  decreases monotonically with transmit power beyond  $P_{\eta_{EE}}^*$ . Hence, the Property 2 can be easily verified.

The maximisation problem (15a) is an integer combinatorial fractional programming problem and is generally NP-hard. For better tractability, we first relax the integer variables,  $\sigma_{k,n}^{(m)} \in \{0, 1\}$  into continuous variables,  $\tilde{\sigma}_{k,n}^{(m)} \in [0, 1]$ . Then, the modified problem for (15a) can be written as

$$\eta = \max_{\tilde{\sigma}_{k,n}^{(m)}, p_{k,n}^{(m)}} \eta_{EE} \left( 1 + \alpha \left( \frac{\theta_{SE} \times \eta_{SE}}{\theta_{EE} \times \eta_{EE}} \right) \right), \quad (16a)$$

$$\text{s.t. (13b) - (13e).} \quad (16b)$$

$$\alpha \geq 0, \quad p_{k,n}^{(m)} \geq 0, \quad \tilde{\sigma}_{k,n}^{(m)} \in [0, 1], \quad \forall n, \forall k, \forall m. \quad (16c)$$

*Lemma 1:*  $\eta$  is jointly quasi-concave with respect to  $p_{k,n}^{(m)}$  and  $\tilde{\sigma}_{k,n}^{(m)}$ .

*Proof:* Please refer to the **Appendix A**.

$\eta$  is quasi-concave with respect to the optimisation variables and a unique optimal solution can be obtained using convex optimisation techniques such as bisection method

and Lagrangian dual decomposition method [36]. As mentioned in [37] and [38], any sum-of-ratios (or fractional form) optimisation problem can be transformed into an equivalent optimisation problem in sum-of-ratios subtractive form. It has been proven in [37, Th. 1] that problems (16a) and (17) are equivalent to each other, i.e., the solution of (17) corresponds to the optimal transmission power. As a result, we will focus on the equivalent subtractive objective function in the rest of the paper. Hence, the non-linear fractional optimisation problem in (16a) can be transformed into the parameterized function as

$$G(\eta) = \left( \underbrace{\sum_{m \in \mathcal{M}} \sum_{k \in \mathcal{K}_m} \sum_{n \in \mathcal{N}} r_{k,n}^{(m)} \left( 1 + \alpha \left( \frac{\theta_{SE} P}{\theta_{EE} B} \right) \right)}_{\text{First term}} - \underbrace{\eta \left( N \times P_C + \epsilon_0 \sum_{m \in \mathcal{M}} \sum_{k \in \mathcal{K}_m} \sum_{n \in \mathcal{N}} \tilde{\sigma}_{k,n}^{(m)} p_{k,n}^{(m)} \right)}_{\text{Second term}} \right). \quad (17)$$

*Remark 2:* The concavity of transformed objective function in (17) with respect to the optimisation variables  $\tilde{\sigma}_{k,n}^{(m)}$  and  $p_{k,n}^{(m)}$  can be proved in two steps. Firstly, we prove the concavity of first term in (17) with respect to the optimisation variables  $\tilde{\sigma}_{k,n}^{(m)}$  and  $p_{k,n}^{(m)}$ . For notational simplicity, we define a vector  $z_{k,n}^{(m)} = [\tilde{\sigma}_{k,n}^{(m)} \quad p_{k,n}^{(m)}]$  and a function  $f_{k,n}^{(m)}(z_{k,n}^{(m)}) = r_{k,n}^{(m)} \left( 1 + \alpha \left( \frac{\theta_{SE} P}{\theta_{EE} B} \right) \right)$  which takes  $z_{k,n}^{(m)}$  as an input. The Hessian matrix  $H(f_{k,n}^{(m)}(z_{k,n}^{(m)}))$  of  $f_{k,n}^{(m)}(z_{k,n}^{(m)})$  is a negative semi-definite matrix and its corresponding both eigenvalues are also negative. Therefore,  $f_{k,n}^{(m)}(z_{k,n}^{(m)})$  is jointly concave with respect to the optimisation variables  $\tilde{\sigma}_{k,n}^{(m)}$  and  $p_{k,n}^{(m)}$ . Subsequently,  $\sum_{m \in \mathcal{M}} \sum_{k \in \mathcal{K}_m} \sum_{n \in \mathcal{N}} r_{k,n}^{(m)} \left( 1 + \alpha \left( \frac{\theta_{SE} P}{\theta_{EE} B} \right) \right)$  is also concave since it is the linear combination of  $f_{k,n}^{(m)}(z_{k,n}^{(m)})$  which preserves the concavity. Finally,  $\left( N \times P_C + \epsilon_0 \sum_{m \in \mathcal{M}} \sum_{k \in \mathcal{K}_m} \right.$

$\left. \sum_{n \in \mathcal{N}} \tilde{\sigma}_{k,n}^{(m)} p_{k,n}^{(m)} \right)$  is an affine function with respect to the optimisation variables  $\tilde{\sigma}_{k,n}^{(m)}$  and  $p_{k,n}^{(m)}$ . Therefore, it is proved that  $G(\eta)$  is jointly concave with respect to the optimisation variables  $\tilde{\sigma}_{k,n}^{(m)}$  and  $p_{k,n}^{(m)}$ . As a result, strong duality holds and solving the dual problem is equivalent to solving the primal problem of (17). It has been shown that the duality gap approaches to zero for sufficiently large number of subcarriers and it is quite small for practical number of subcarriers as mentioned in [39] and [40]. In [40], it is shown that only 8 subcarriers are sufficient in some cases to achieve zero duality gap.

It is worth to mention that  $G(\eta)$  monotonically decreases with an increase in  $\eta$ , i.e.,  $G(\eta') > G(\eta)$  if  $\eta' > \eta$ . The optimal solution  $\eta = \eta^*$  of (17) can be determined by finding the root to the  $G(\eta)$ , i.e., the transformed fractional form in subtractive form of (16a), using various root finding methods [36].

**Lemma 2:**  $\mathcal{G}(\eta) \triangleq \max_{\tilde{\sigma}_{k,n}^{(m)}, p_{k,n}^{(m)}} G(\eta)$  under the constraints (16b) – (16c), satisfies

$$\mathcal{G}(\eta) = 0 \text{ iff } \eta = \eta^*.$$

From Lemma 2,  $\mathcal{G}(\eta)$  is strictly monotonically decreasing with respect to  $\eta$ . The lemma also implies that when  $\eta \rightarrow -\infty, \mathcal{G}(\eta) > 0$  and when  $\eta \rightarrow \infty, \mathcal{G}(\eta) < 0$ . (17) shows that  $G(\eta) > 0$ , when  $\eta \leq 0$ , because the first and second terms in (17) are definitely positive. Therefore,  $G(\eta) = 0$  occurs at  $\eta > 0$ , and hence, we will solve (17) for  $\eta > 0$ . Details of its proof can be found in **Appendix B**.

#### IV. EE AND SE TRADEOFF RESOURCE ALLOCATION SCHEME

In HetNets, there exists two different channel deployment schemes, co-channel and orthogonal channel deployment schemes. In the former scheme, the macrocell and a set of pico BSs are permitted to use the same resource for data transmission at any time, which will cause co-tier and cross-tier interference. In orthogonal channel deployment scheme, the spectrum is divided into two orthogonal parts, one part for macrocell use and the second part for the set of pico BSs such that each resource is exclusively assigned to either macrocell  $m_0$  or a set of pico BSs  $m_i, \forall i \in \{1, 2, \dots, M - 1\}$ , at any time causing no cross-tier interference between macrocell and the set of pico BSs. The co-tier interference will still occur among those pico BSs sharing the same resources. However, in this paper we consider co-channel deployment scheme such that co-tier interference is assumed to be part of thermal noise  $N_0$  as discussed earlier in section II.

In this section, we proposed an iterative algorithm for solving (17) with an equivalent subtractive objective function such that the obtained solution satisfies the conditions stated in Lemma II. The solution to the EE-SE tradeoff problem is formulated as a two-layer solution. We have proposed an iterative Dinkelbach type method<sup>2</sup> (Algorithm-1) as an outer layer solution to find an optimal solution to (17) by determining a root to  $G(\eta) = 0$ . Note that for any value of  $\eta$ , generated by Algorithm-1 in each iteration,  $G(\eta) \geq 0$  is always valid; negative utility value will not occur. In particular,  $\sum_{m \in \mathcal{M}} \sum_{k \in \mathcal{K}_m} \sum_{n \in \mathcal{N}} r_{k,n}^{(m)} \left(1 + \alpha \left(\frac{\theta_{SE} P}{\theta_{EE} B}\right)\right)$  represents the system utility due to the data transmission while  $\eta \left(N \times P_C + \epsilon_0 \sum_{m \in \mathcal{M}} \sum_{k \in \mathcal{K}_m} \sum_{n \in \mathcal{N}} \tilde{\sigma}_{k,n}^{(m)} p_{k,n}^{(m)}\right)$  represents the associated cost due to the energy consumption. The optimal value of  $\eta$  indicates a scaling factor for balancing the

<sup>2</sup>It is an application of Newton method to find the root of an objective function.

#### Algorithm 1 Iterative EE and SE Tradeoff Algorithm

**Initialize**

$iter = \text{max number of iterations}, \Delta = \text{maximum acceptable tolerance},$

Set  $i=1$  and  $\eta(1) = 0,$

**While**  $(|G(\eta)| < \Delta) \parallel (i < iter)$  **do**

Solve (17) for a given value of  $\eta(i)$  using Algorithm-2.

$$\text{Update } \eta(i+1) = \frac{\left(\sum_{m \in \mathcal{M}} \sum_{k \in \mathcal{K}_m} \sum_{n \in \mathcal{N}} r_{k,n}^{(m)} \left(1 + \alpha \frac{\tau_{EE}}{\tau_{SE}}\right)\right)}{\left(N \times P_C + \epsilon_0 \sum_{m \in \mathcal{M}} \sum_{k \in \mathcal{K}_m} \sum_{n \in \mathcal{N}} \tilde{\sigma}_{k,n}^{(m)} p_{k,n}^{(m)}\right)}$$

Update  $i = i + 1$

**end While**

**Output:**  $[\eta]$

system utility and cost. At an iteration  $i - 1$ , the value of  $\eta$  is initialised and the  $G(\eta)$  is solved for a given value of  $\eta$ , i.e.,  $\eta_{i-1}$ , and the optimal power  $p_{i-1}^*$  is computed using the dual decomposition approach, i.e., inner layer solution, explained in the next section. The optimal power computed in iteration  $i - 1$  can be used to update the value of  $\eta$  for iteration  $i$ . This process is repeated until it converges to an optimal value  $\eta^*$ . The proof of convergence for the proposed method is guaranteed and its pseudo code is shown in Algorithm-1. In particular,  $\eta$  increases in each iteration  $i$  such that  $\eta_{i+1} > \eta_i$ . For a large number of iterations  $iter$ ,  $\eta$  converges to an optimal value  $\eta^*$  such that it satisfies the optimality condition in **Lemma 2**, i.e.,  $G(\eta) = 0$ . The proof of the convergence can be achieved using a similar approach as mentioned in [37, Appendix A] and [38] and is not provided here due to the space limitations.

#### A. DUAL DECOMPOSITION FORMULATION

In this subsection, we solve the tradeoff optimisation problem by solving its dual to the primal problem for a given value of  $\eta$ . By using the dual decomposition approach [37], [39], an iterative procedure can be obtained to solve  $G(\eta) = 0$  in each iteration of the proposed Algorithm-1. It is shown that the dual decomposition approach has lower computational complexity as compared to the exhaustive search or the branch-and-bound schemes [41]. In order to apply dual decomposition method, the Lagrangian function of (17) using standard convex optimisation methods as mentioned in [36] can be written as follow:

$$\begin{aligned} L(p, \lambda, \underline{\mu}, \underline{\nu}) = & \sum_{m \in \mathcal{M}} \sum_{k \in \mathcal{K}_m} \sum_{n \in \mathcal{N}} r_{k,n}^{(m)} \left(1 + \alpha \frac{\tau_{EE}}{\tau_{SE}}\right) \\ & - \eta \left(\epsilon_0 \sum_{m \in \mathcal{M}} \sum_{k \in \mathcal{K}_m} \sum_{n \in \mathcal{N}} \tilde{\sigma}_{k,n}^{(m)} p_{k,n}^{(m)} + N \times P_C\right) \\ & + \sum_{n \in \mathcal{N}} \lambda_n \left(\sum_{m \in \mathcal{M}} \sum_{k \in \mathcal{K}_m} r_{k,n}^{(m)} - R_n^{\min}\right) \end{aligned}$$

$$\begin{aligned}
 & + \sum_{n \in \mathcal{N}} \mu_n \left( P_n^{\max} - \sum_{m \in \mathcal{M}} \sum_{k \in \mathcal{K}_m} \tilde{\sigma}_{k,n}^{(m)} P_{k,n}^{(m)} \right) \\
 & + \sum_{k \in \mathcal{K}_m} \nu_k \left( I_k^{\text{th}} - \sum_{m \in \mathcal{M}} \sum_{n \in \mathcal{N}_m} \tilde{\sigma}_{k,n}^{(m)} P_{k,n}^{(m)} g_{k,n}^{mm_0} \right)
 \end{aligned} \quad (18)$$

where  $\tau_{\text{EE}} = \frac{P}{\theta_{\text{EE}}}$  and  $\tau_{\text{SE}} = \frac{B}{\theta_{\text{SE}}}$ .  $\underline{\lambda} = (\lambda_1, \lambda_2, \dots, \lambda_N)$  is the Lagrange multiplier vector associated with the minimum data rate constraint (13b).  $\underline{\mu} = (\mu_1, \mu_2, \dots, \mu_N)$  is the Lagrange multiplier vector associated with the total transmit power constraint (13c).  $\underline{\nu} = (\nu_1, \nu_2, \dots, \nu_K)$  is the Lagrange multiplier vector corresponding to the cross-tier interference constraint (13d) and  $\nu_k = 0$  for  $k \in \mathcal{K}_{m_0}$ . The constraints in (13e) and (16c) are later considered by dual decomposition method such that each subcarrier can be exclusively assigned to a single user within a network  $m$  and the non-negative optimal powers are computed. The dual problem corresponding to the primal problem of (17) can be given by [42]:

$$\min_{\underline{\lambda}, \underline{\mu}, \underline{\nu} \geq 0} \max_{\sigma, p} L(p, \underline{\lambda}, \underline{\mu}, \underline{\nu}) \quad (19)$$

The Lagrange dual function corresponding to problem (17) is

$$g(\underline{\lambda}, \underline{\mu}, \underline{\nu}) = \max_{\sigma, p} L(p, \underline{\lambda}, \underline{\mu}, \underline{\nu}) \quad (20)$$

Similarly,  $g(\underline{\lambda}, \underline{\mu}, \underline{\nu})$  is the dual function and can be shown as

$$\begin{aligned}
 g(\underline{\lambda}, \underline{\mu}, \underline{\nu}) & = \sum_{k \in \mathcal{K}_m} g_k(\underline{\lambda}, \underline{\mu}, \underline{\nu}) - \eta \varepsilon_0 N P_C - \sum_{n \in \mathcal{N}} \lambda_n R_n^{\min} \\
 & + \sum_{n \in \mathcal{N}} \mu_n P_n^{\max} + \sum_{k \in \mathcal{K}} \nu_k I_k^{\text{th}}, \quad (21)
 \end{aligned}$$

where  $g_k(\underline{\lambda}, \underline{\mu}, \underline{\nu})$  is defined by

$$\begin{aligned}
 & g_k(\underline{\lambda}, \underline{\mu}, \underline{\nu}) \\
 & = \max_{\tilde{\sigma}_{k,n}, p_k} \left( \sum_{m \in \mathcal{M}} \sum_{n \in \mathcal{N}} r_{k,n}^{(m)} \left( 1 + \alpha \frac{\tau_{\text{EE}}}{\tau_{\text{SE}}} \right) - \eta \varepsilon_0 \sum_{m \in \mathcal{M}} \sum_{n \in \mathcal{N}} \right. \\
 & \quad \tilde{\sigma}_{k,n}^{(m)} P_{k,n}^{(m)} + \sum_{m \in \mathcal{M}} \sum_{n \in \mathcal{N}} \lambda_n r_{k,n}^{(m)} - \sum_{m \in \mathcal{M}} \sum_{n \in \mathcal{N}} \\
 & \quad \left. \mu_n \tilde{\sigma}_{k,n}^{(m)} P_{k,n}^{(m)} - \sum_{m \in \mathcal{M}} \sum_{n \in \mathcal{N}_m} \nu_k \tilde{\sigma}_{k,n}^{(m)} P_{k,n}^{(m)} g_{k,n}^{mm_0} \right) \quad (22)
 \end{aligned}$$

The corresponding dual problem to the primal problem of (17) is hence given by

$$\begin{aligned}
 & \min_{\underline{\lambda}, \underline{\mu}, \underline{\nu}} g(\underline{\lambda}, \underline{\mu}, \underline{\nu}) \\
 & \text{s.t. } \underline{\lambda} \geq 0, \quad \underline{\mu} \geq 0, \quad \underline{\nu} \geq 0 \quad (23)
 \end{aligned}$$

## B. DUAL DECOMPOSITION SOLUTION

To solve the dual problem in (19), we have decomposed it into a hierarchy of two problems. The slave problem is an inner maximisation in (20) consisting of  $K$  subproblems solved in parallel to compute the power and subcarrier allocation on each subcarrier  $k \in \mathcal{K}$  for the given values of  $\lambda, \mu, \nu$  and  $\eta$ ; whereas an outer minimisation in (23) is the master problem in which the Lagrangian multipliers are updated using a sub-gradient method. After a few mathematical manipulations, (22) can be written as

$$\begin{aligned}
 g_k(\underline{\lambda}, \underline{\mu}, \underline{\nu}) & = \max_{\tilde{\sigma}_{k,n}, p_k} \left( \sum_{m \in \mathcal{M}} \sum_{n \in \mathcal{N}} \tilde{\sigma}_{k,n}^{(m)} B_k \log_2 \left( 1 + \gamma_{k,n}^{(m)} P_{k,n}^{(m)} \right) \right. \\
 & \quad \times \left[ \left( 1 + \alpha \frac{\tau_{\text{EE}}}{\tau_{\text{SE}}} \right) + \lambda_n \right] - \sum_{m \in \mathcal{M}} \sum_{n \in \mathcal{N}} \\
 & \quad \left. \left( \mu_n + \eta \varepsilon_0 + \nu_k g_{k,n}^{mm_0} \right) \tilde{\sigma}_{k,n}^{(m)} P_{k,n}^{(m)} \right) \quad (24)
 \end{aligned}$$

Now, by taking the first-order derivatives of (24) with respect to  $\tilde{\sigma}_{k,n}^{(m)}$ , we get

$$\begin{aligned}
 \frac{\partial g_k(\underline{\lambda}, \underline{\mu}, \underline{\nu})}{\partial \tilde{\sigma}_{k,n}^{(m)}} & = B_k \log_2 \left( 1 + \gamma_{k,n}^{(m)} P_{k,n}^{(m)} \right) \left[ \left( 1 + \alpha \frac{\tau_{\text{EE}}}{\tau_{\text{SE}}} \right) + \lambda_n \right] \\
 & - \left( \mu_n + \eta \varepsilon_0 + \nu_k g_{k,n}^{mm_0} \right) P_{k,n}^{(m)} \quad (25)
 \end{aligned}$$

The subcarrier assignment index  $\tilde{\sigma}_{k,n}^{(m)}$  at given  $\lambda, \mu, \nu$  and  $\eta$  can be determined as:

$$\tilde{\sigma}_{k,n}^{(m)} = \begin{cases} 1, & \text{if } (k, m^*, n^*) = \arg \max_{m,n} B_k \\ \log_2 \left( 1 + \gamma_{k,n}^{(m)} P_{k,n}^{(m)} \right) \left[ \left( 1 + \alpha \frac{\tau_{\text{EE}}}{\tau_{\text{SE}}} \right) + \lambda_n \right] \\ \quad - \left( \mu_n + \eta \varepsilon_0 + \nu_k g_{k,n}^{mm_0} \right) P_{k,n}^{(m)} \\ 0, & \text{otherwise.} \end{cases} \quad (26)$$

Note that (26) also gives us an insight into the user association and the set of subcarriers assigned to the network  $m$ , i.e.,  $\mathcal{K}_m$ , which consists of all the subcarriers  $k \in \mathcal{K}$  with  $\tilde{\sigma}_{k,n}^{(m)} = 1$ . For a fixed set of Lagrange multipliers and a given parameter  $\eta$ , the power for user  $n$  on subcarrier  $k$  can be computed by taking the first-order derivative of (24) with respect to  $p_{k,n}^{(m)}$ , yielding

$$\begin{aligned}
 \frac{\partial g_k(\underline{\lambda}, \underline{\mu}, \underline{\nu})}{\partial p_{k,n}^{(m)}} & = \frac{\tilde{\sigma}_{k,n}^{(m)} B_k \left[ \left( 1 + \alpha \frac{\tau_{\text{EE}}}{\tau_{\text{SE}}} \right) + \lambda_n \right] \times \gamma_{k,n}^{(m)}}{\ln(2) \left( 1 + \gamma_{k,n}^{(m)} P_{k,n}^{(m)} \right)} \\
 & - \left( \mu_n + \eta \varepsilon_0 + \nu_k g_{k,n}^{mm_0} \right) \quad (27)
 \end{aligned}$$

Applying the KKT conditions results in

$$\left. \frac{\partial g_k(\underline{\lambda}, \underline{\mu}, \underline{\nu})}{\partial p_{k,n}^{(m)}} \right|_{p_{k,n}^{(m)} = p_{k,n}^{(m)*}} = 0 \implies$$

Hence,

$$p_{k,n}^{(m)} = \begin{cases} \left( \frac{B_k \left( (1 + \alpha \frac{\tau_{EE}}{\tau_{SE}}) + \lambda_n \right)}{\ln 2 \left( \mu_n + \eta \varepsilon_0 + \nu_k g_{k,n}^{mm_0} \right)} - \frac{1}{\gamma_{k,n}^{(m)}} \right)^+, & \text{if } \tilde{\sigma}_{k,n}^{(m)} = 1. \\ 0, & \text{otherwise.} \end{cases} \quad (28)$$

The optimal solution of (17) can then be expressed as

$$p_{k,n}^{(m)*} = \max \left( \min \left( p_{k,n}^{(m)}, P_n^{\max} \right), P_n^{\min} \right), \quad (29)$$

where  $P_n^{\min} = \left( 2^{\left( \sigma_{k,n}^{(m)} R_n^{\min} / B_k \right)} - 1 \right) / \gamma_{k,n}^{(m)}$ . Thus, the optimal power allocation for each user  $n$  on subcarrier  $k$  has a semi-closed form expression in terms of dual variables  $\lambda$ ,  $\mu$  and  $\nu$ . We also observe that the optimal power allocation given by (28) is a modified water filling solution, where the channel gain is given by  $\gamma_{k,n}^{(m)}$  and the water levels are determined both by the Lagrangian multipliers  $\lambda$ ,  $\mu$ ,  $\nu$  and weighting coefficient  $\alpha$  as well by the EE-SE tradeoff metric  $\eta$ . The dual variables  $\{\underline{\lambda}, \underline{\mu}, \underline{\nu}\}$  must satisfy the KKT conditions in order to be optimal and  $\tilde{\sigma}_{k,n}^{(m)} = 1$  indicates that the subcarrier  $k$  is assigned to user  $n$  associated with network  $m$ .

It should be noted that the weighted coefficient  $\alpha = 0$  maximises the EE whereas at  $\alpha = \alpha_{SE}$  the SE is maximised. For a given subcarrier assignment, the SE is maximised when each user transmits at their maximum transmission power. We assume that each user distribute its maximum transmission power equally among its subcarriers such that  $p_{k,n}^{(m)} = \frac{P_n^{\max}}{|K_n|}$ , where  $K_n$  is the set of subcarriers allocated to user  $n$ . In order to compute the weighted coefficient  $\alpha_{SE}^{(n)}$  which can achieve the maximum SE for user  $n$ , (28) can be rewritten as:

$$\frac{P_n^{\max}}{|K_n|} = \left( \frac{B_k \left( (1 + \alpha_{SE}^{(n)} \frac{\tau_{EE}}{\tau_{SE}}) + \lambda_n \right)}{\ln 2 \left( \mu_n + \eta \varepsilon_0 + \nu_k g_{k,n}^{mm_0} \right)} - \frac{1}{\gamma_n^{\min}} \right), \quad (30)$$

where  $\gamma_n^{\min}$  is the minimum channel-to-noise-ratio (CNR) among all the subcarriers allocated to the user  $n$ . From (30),  $\alpha_{SE}^{(n)}$  can be easily derived as:

$$\alpha_{SE}^{(n)} = \frac{\tau_{SE}}{\tau_{EE}} \left[ \left( \frac{P_n^{\max}}{|K_n|} + \frac{1}{\gamma_n^{\min}} \right) \times \frac{\ln 2 \left( \mu_n + \eta \varepsilon_0 + \nu_k g_{k,n}^{mm_0} \right)}{B_k} - \lambda_n - 1 \right]. \quad (31)$$

Finally,  $\alpha_{SE}$  can be computed as

$$\alpha_{SE} = \max \{ \alpha_{SE}^{(1)}, \alpha_{SE}^{(2)}, \dots, \alpha_{SE}^{(N)} \}. \quad (32)$$

### C. UPDATING THE DUAL VARIABLES

In order to minimise the dual function  $g(\underline{\lambda}, \underline{\mu}, \underline{\nu})$ , since the dual function is differentiable the subgradient method can be used to update the dual variables  $\lambda$ ,  $\mu$  and  $\nu$ . The subgradient

of  $\lambda$ ,  $\mu$  and  $\nu$  are respectively given by taking the derivative of  $L(p, \underline{\lambda}, \underline{\mu}, \underline{\nu})$  with respect to  $\lambda$ ,  $\mu$  and  $\nu$ , yielding

$$\Delta \lambda = \sum_{m \in \mathcal{M}} \sum_{k \in \mathcal{K}_m} r_{k,n}^{(m)} - R_n^{\min}, \quad (33a)$$

$$\Delta \mu = P_n^{\max} - \sum_{m \in \mathcal{M}} \sum_{k \in \mathcal{K}_m} p_{k,n}^{(m)}. \quad (33b)$$

$$\Delta \nu = I_{th}^{(k)} - \sum_{\substack{m \in \mathcal{M} \\ m \neq m_0}} \sum_{n \in \mathcal{N}_m} \tilde{\sigma}_{k,n}^{(m)} p_{k,n}^{(m)} g_{k,n}^{mm_0}. \quad (33c)$$

Then, we can update the Lagrange multipliers  $(\lambda, \mu)$  according to

$$\lambda_n(i+1) = \left[ \lambda_n(i) - \frac{s^1}{\sqrt{i}} \left( \sum_{m \in \mathcal{M}} \sum_{k \in \mathcal{K}_m} r_{k,n}^{(m)} - R_n^{\min} \right) \right]^+, \quad \forall n \quad (34a)$$

$$\mu_n(i+1) = \left[ \mu_n(i) - \frac{s^2}{\sqrt{i}} \left( P_n^{\max} - \sum_{m \in \mathcal{M}} \sum_{k \in \mathcal{K}_m} p_{k,n}^{(m)} \right) \right]^+, \quad \forall n \quad (34b)$$

$$\nu_k(i+1) = \left[ \nu_k(i) - \frac{s^3}{\sqrt{i}} \times \left( I_{th}^{(k)} - \sum_{\substack{m \in \mathcal{M} \\ m \neq m_0}} \sum_{n \in \mathcal{N}_m} \tilde{\sigma}_{k,n}^{(m)} p_{k,n}^{(m)} g_{k,n}^{mm_0} \right) \right]^+, \quad \forall k \quad (34c)$$

Here,  $i$  is the iteration number and  $s^l = \frac{0.1}{\sqrt{i}}$ ,  $l \in \{1, 2, 3\}$  are the positive step sizes assumed in this paper. The process of computing the optimal power allocation and Lagrangian multipliers are updated accordingly until the convergence is achieved, indicating that the dual optimal point is achieved. The subgradient update is guaranteed to converge to optimal values of  $\lambda$ ,  $\mu$  and  $\nu$ , as long as  $s^l$  is chosen to be sufficiently small [36]. A common practice is to choose square summable step sizes in contrast to absolute step sizes [39], [42].

### D. COMPLEXITY ANALYSIS

The computational complexity of the proposed approach depends on the complexity of both inner and outer layer solutions. We observe that the computational complexity of Algorithm-1 to solve all  $K$  independent subproblems in (21), to solve  $g(\underline{\lambda}, \underline{\mu}, \underline{\nu})$  is  $O(KN)$ . In addition, with the accuracy requirement, i.e.,  $|U(\eta(i)) - U(\eta(i-1))| < \Delta$ , set in Algorithm-2, the total computational complexity of our proposed approach is approximately  $O\left(C_\eta KN \log_2\left(\frac{1}{\Delta}\right)\right)$ , where  $C_\eta$  is the number of iterations required for updating  $\eta$  until Algorithm-1 converges. It is demonstrated in the simulation results that less than 5 iterations are needed for Algorithm-1 to converge. The proposed approach has polynomial complexity regarding the problem scale  $K$  and  $N$ , which is attractive in the practical OFDMA implementation.

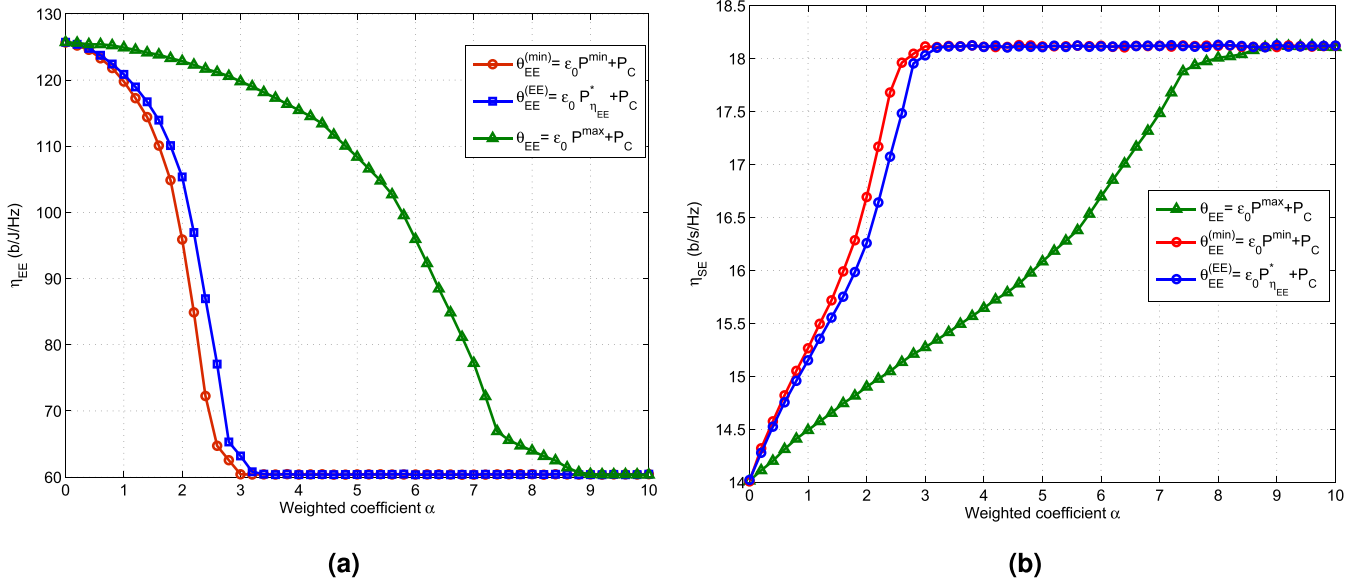


FIGURE 2. EE and SE versus  $\alpha$  for various  $\theta_{EE}$  with  $\theta_{SE} = B$ ,  $N = 10$ ,  $K = 10$ ,  $P^{\max} = 0.2W$  and  $P_C = 0.1W$ . (a) EE as a function of weighted coefficient alpha. (b) SE as a function of weighted coefficient alpha.

**Algorithm 2** Joint User Association, Subcarrier and Power Allocation

**Input:**  $[\eta, \alpha, \epsilon_0, \gamma_{k,n}^{(m)}]$   
**Step 1: Initialize**  
 $i = 0, p_{k,n}^{(m)} = 0, \lambda_n^{(i)} = 0.001, \mu_n^{(i)} = 0.01, v_k^{(i)} = 0.001,$   
**for**  $n = 1, \dots, N, k = 1, \dots, K, m = 1, 2, \dots, M.$   
**Step 2:**  
**For**  $n = 1 : N$   
**For**  $k = 1 : K$   
 Calculate  $p_{k,n}^{(m)}$  according to (28).  
**end For**  
 Obtain the user association and subcarrier assignment according to (26).  
**end For**  
**Step 3:**  
 $i=i+1$   
 Update  $\lambda_n^{(i+1)}, \mu_n^{(i+1)}$  and  $v_k^{(i+1)}$  according to (34).  
**Step 4:**  
 Repeat steps (2)-(3) until  $\lambda_n^{(i+1)}, \mu_n^{(i+1)}$  and  $v_k^{(i+1)}$  are converged.  
**Output:**  $[p_{k,n}^{(m)}, \tilde{\sigma}_{k,n}^{(m)}]$

Therefore, we can conclude that the computational complexity of the proposed approach is low and acceptable.

**V. SIMULATION RESULTS**

We consider a two-tier HetNets environment with a single macrocell with 500 m radius overlaid with  $M - 1$  pico BSs with a radius of 50 m. The bandwidth of each subcarrier is 30 kHz. The maximum transmission power for all users are the same, hence,  $P_n^{\max}$  will be referred to as  $P^{\max}$ . Similarly, the minimum rate requirement  $R_n^{\min}$  can be referred

to as  $R^{\min}$ . The minimum-rate requirement for each user is considered to be 4 b/s/Hz unless stated otherwise. The maximum transmission power of users considered in the simulation vary from 200mW to 500mW, whereas the value of circuit power of users is set fixed to  $P_C = 100mW$  and the threshold interference level is assumed as  $I_n^{\text{th}} = 1.1943 \times 10^{-14}$  W, unless stated otherwise. We assume that the users are uniformly deployed within the simulated scenario. The path-loss model for macrocell and pico BS  $m_i$  are given as  $PL_n^{(m_0)}(\text{dB}) = 128.1 + 37.6 \log_{10}(d_n)$  and  $PL_n^{(m_i)}(\text{dB}) = 140.7 + 36.7 \log_{10}(d_n)$  [2], where  $d_n$  is the distance of user  $n$  from the serving BS in km, and therefore,  $PL_n^{(m_0)} = 10^{(PL_n^{(m_0)}(\text{dB})/10)}$  and  $PL_n^{(m_i)} = 10^{(PL_n^{(m_i)}(\text{dB})/10)}$ . The noise spectral density is assumed to be  $N_0 = -174$  dBm/Hz. In this work, the power amplifier efficiency is assumed as 38%, i.e.,  $\epsilon_0 = \frac{1}{0.38}$ . Note that if the user is unable to meet the minimum rate requirement  $R^{\min}$ , or the maximum transmission power constraint  $P^{\max}$ , we set the EE and SE for that channel realisation to zero. All the simulation results presented in this section are averaged over  $10^6$  independent network realizations.

The initial selections of  $\theta_{EE}$  and  $\theta_{SE}$  are critical to the overall performance of the EE-SE tradeoff in HetNets. Fig. 2 illustrates the impact of different notions of normalization factor  $\theta_{EE}$  on the achievable EE and achievable SE in Figs. 2(a) and 2(b), respectively. First, we fix the value of  $\theta_{SE}$ , the proposed notions of  $\theta_{EE}$  is depicted with both minimum transmission power  $P^{\min}$  ( $\theta_{EE}^{(\min)} = \epsilon_0 P^{\min} + P_C$ ), maximum transmission power  $P^{\max}$  ( $\theta_{EE}^{(\max)} = \epsilon_0 P^{\max} + P_C$ ), and with the energy-efficient transmission power  $P_{\eta_{EE}}^*$  ( $\theta_{EE}^{(EE)} = \epsilon_0 P_{\eta_{EE}}^* + P_C$ ), as the benchmark case. For the  $\theta_{EE}^{(\min)}$  case,  $P^{\min}$  is the minimum

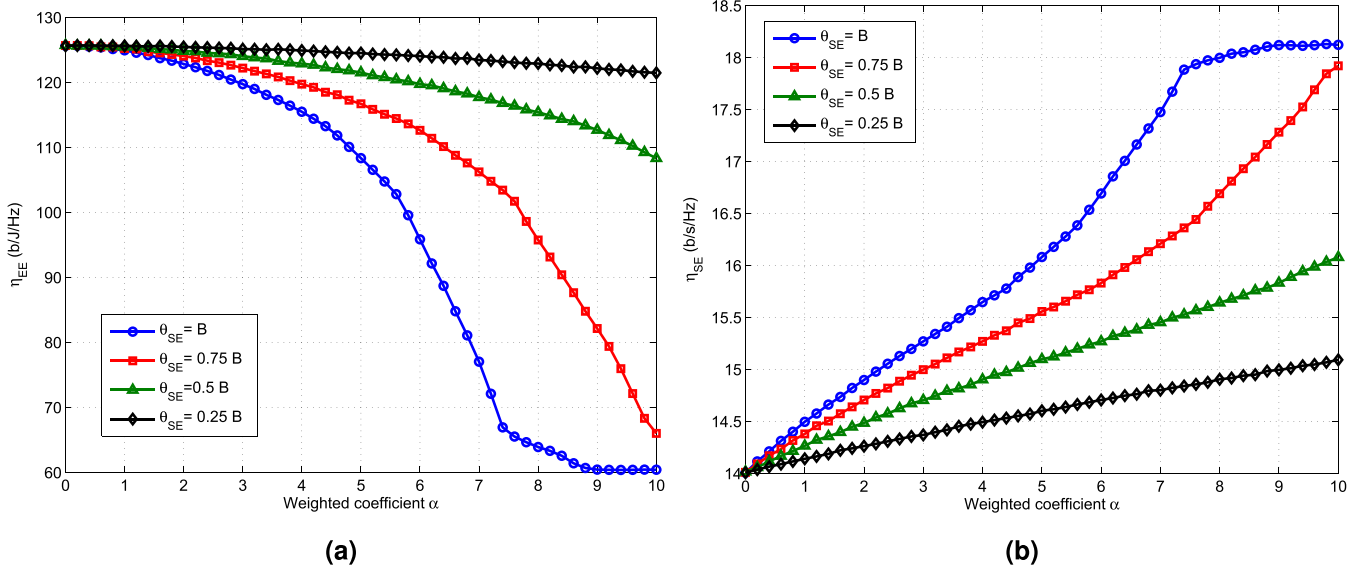


FIGURE 3. EE and SE versus  $\alpha$  for various  $\theta_{SE}$  with  $\theta_{EE} = (\epsilon_0 P^{\max} + P_C)$ ,  $N = 10$ ,  $K = 10$ ,  $P^{\max} = 0.2W$  and  $P_C = 0.1W$ .

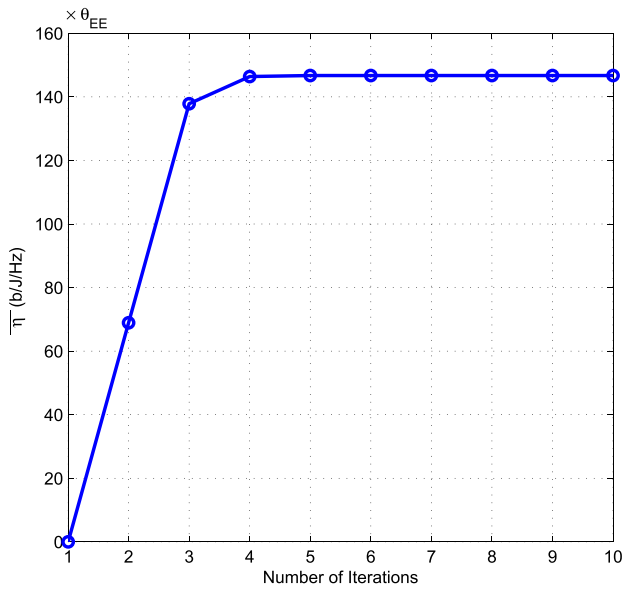
transmission power required to achieve the minimum rate requirement  $R^{\min}$  which lies in the set of  $[0, P^{\max}]$ . For the benchmark case,  $P_{\eta_{EE}}^*$  is the energy-efficient transmission power at which the maximum EE is achieved and it lies in the set of  $[P^{\min}, P^{\max}]$ . The optimal transmit power  $P_{\eta}^*$  monotonically increases with  $\alpha$  regardless of  $\theta_{EE}$ .  $P_{\eta}^*$  achieves the maximum transmission power  $P^{\max}$  at  $\alpha \approx 3$  and  $\alpha \approx 3.2$  for the proposed  $\theta_{EE}^{(\min)}$  and benchmark cases, respectively. On the other hand,  $P_{\eta}^*$  achieves the maximum transmission power  $P^{\max}$  at  $\alpha \approx 9$  for the proposed  $\theta_{EE}^{(\max)}$  case. For the weighted coefficient  $0 \leq \alpha \leq 0.6$ , the achieved EE for all three cases are marginally close to each other whereas as the value of  $\alpha$  increases beyond 0.6 the achieved EE by the proposed  $\theta_{EE}^{(\max)}$  is far higher as compared to the proposed  $\theta_{EE}^{(\min)}$  and benchmark cases. The figure shows that in  $\theta_{EE}^{(\max)}$  case, the achieved EE decreases more gradually with  $\alpha$ , when compared to the  $\theta_{EE}^{(\min)}$  and benchmark cases. After several implementations of our proposed normalization factor, we choose the setting of  $\theta_{EE} = \theta_{EE}^{(\max)} = \epsilon_0 P^{\max} + P_C$  as the optimal  $\theta_{EE}$ . One of the major observation is that optimal  $\theta_{EE}$  provides the complete range of  $\eta_{EE}$  and  $\eta_{SE}$  values as compared to the two baseline cases and gives more flexibility to set preferences for either EE or SE.

Fig. 3 illustrates the impact of  $\theta_{SE}$  on the achievable EE and achievable SE. First, we fix the value of  $\theta_{EE} = \theta_{EE}^{(\max)}$ . The proposed notions of  $\theta_{SE}$  are defined as  $\theta_{SE}^{(\text{tot})}$ ,  $\theta_{SE}^{(1)}$ ,  $\theta_{SE}^{(2)}$  and  $\theta_{SE}^{(3)}$  for  $B$ ,  $0.75B$ ,  $0.5B$  and  $0.25B$  respectively.  $\tau_{SE}$  decreases with  $\theta_{SE}$ , which in turn, reduces  $\alpha \frac{\tau_{EE}}{\tau_{SE}}$  as defined in (18). Hence, for smaller values of  $\theta_{SE}$ , the achieved optimal tradeoff power level  $P_{\eta}^*$  is approximately close to the  $P_{\eta_{EE}}^*$  at  $\alpha = 0$ . For the higher values of  $\theta_{SE}$ , the achieved optimal tradeoff power level  $P_{\eta}^*$  monotonically increases with  $\alpha$  towards the

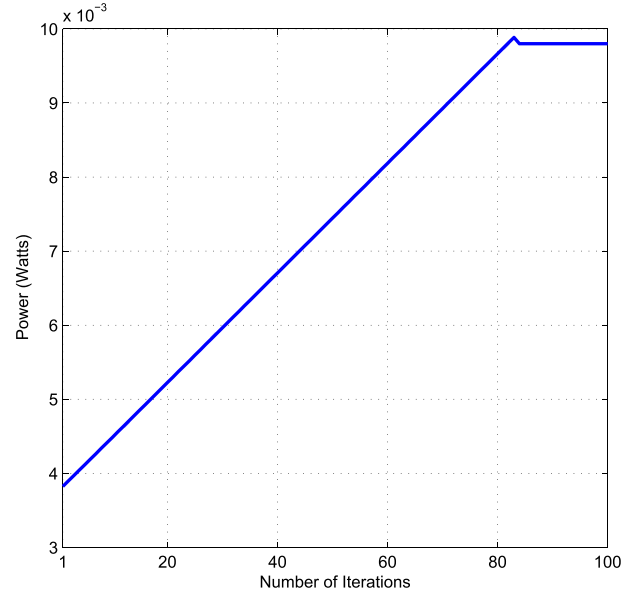
maximum transmission power  $P^{\max}$ . We note that  $P_{\eta}^*$  converges to  $P^{\max}$  at different values of  $\alpha$  depending on the set value of  $\theta_{SE}$ . The figure reveals that for the weighted coefficient  $0 \leq \alpha \leq 2$ , the optimal transmission power and achieved EE for all four cases are approximately close to each other whereas as  $\alpha$  increases beyond 2, the achieved EE by the proposed  $\theta_{SE}^{(\text{tot})}$  is far lower than the remaining three proposed notions of  $\theta_{SE}$ . As  $\theta_{SE}$  is a normalization factor for the achieved SE in the optimisation problem so the optimal  $\theta_{SE}$  is chosen such that it achieves highest SE. After several implementations of our proposed normalization factor, we choose the setting of  $\theta_{SE} = \theta_{SE}^{(\text{tot})} = \sum_{k \in \mathcal{K}} B_k$  as the optimal  $\theta_{SE}$ .

The optimal  $\theta_{SE}$  can achieve a higher SE as compared to the other cases, however, at the cost of reduction in EE. For clarity purpose, from this point onwards  $\theta_{EE}$  and  $\theta_{SE}$  are assumed to be  $\theta_{EE} = \epsilon_0 P^{\max} + P_C$  and  $\theta_{SE} = \sum_{k \in \mathcal{K}} B_k$ .

Fig. 4 depicts the average achieved  $\bar{\eta}$  and the average transmission power versus the number of iterations to study the convergence speed of the proposed Algorithms 1 and 2, respectively. The achieved  $\bar{\eta}$  is corresponding to the objective function defined in (15a). Fig. 4(a) depicts the achieved  $\bar{\eta}$  of the proposed Algorithm 1 versus the number of iterations with the maximum uplink transmission power of  $P^{\max} = 0.2W$ , with the normalisation factors  $\theta_{EE} = 0.63W$ , and  $\theta_{SE} = 3 \times 10^4$  Hz. The algorithm converges to an optimal value within 4-5 iterations. Fig. 4(b), on the other hand, includes the plots for the average transmission power of Algorithm 2 versus the number of iterations. The algorithm converges to an optimal value within around 80 iterations. The polynomial complexity of the proposed Algorithm 1 and 2 depends on the problem scale of the number of users  $N$  and subcarriers  $K$ , which is desirable for practical implementation and has a fast convergence speed. This result demonstrates



(a)



(b)

**FIGURE 4.** Convergence of Proposed Algorithms 1 & 2 with  $\alpha = 1$ ,  $\theta_{SE} = B$ ,  $\theta_{EE} = (\epsilon_0 P^{\max} + P_C)$ ,  $N = 10$ ,  $K = 10$ ,  $P^{\max} = 0.2W$  and  $P_C = 0.1W$ . (a) Algorithm 1. (b) Algorithm 2.

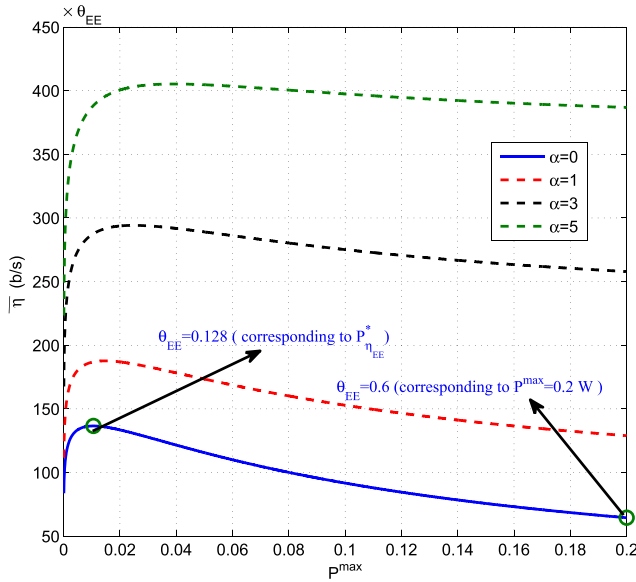


**FIGURE 5.**  $\bar{\eta}$  versus  $P^{\max}$  for various values of  $\alpha$ .

the fact that the proposed Algorithm 1 and 2 guarantee convergence by using the subgradient method in uplink HetNets.

By fixing  $\theta_{SE}$  to  $B$ , the maximum achievable  $\bar{\eta}$  versus  $P^{\max}$  for different values of  $\alpha$  are plotted in Fig. 5 which reveals that  $\bar{\eta}$  increases with  $\alpha$ ; whereas  $\bar{\eta}$  first increases with  $P^{\max}$ , and after a particular value of  $P^{\max}$ , it starts decreasing. This is due to the fact that  $\tau_{EE}$  is defined as  $\frac{P}{\theta_{EE}}$ , where  $\theta_{EE}$  depends on  $P^{\max}$  as defined in (18). For smaller values of  $P^{\max}$ , the achievable  $\bar{\eta}$  increases with  $P^{\max}$ . Furthermore, for higher

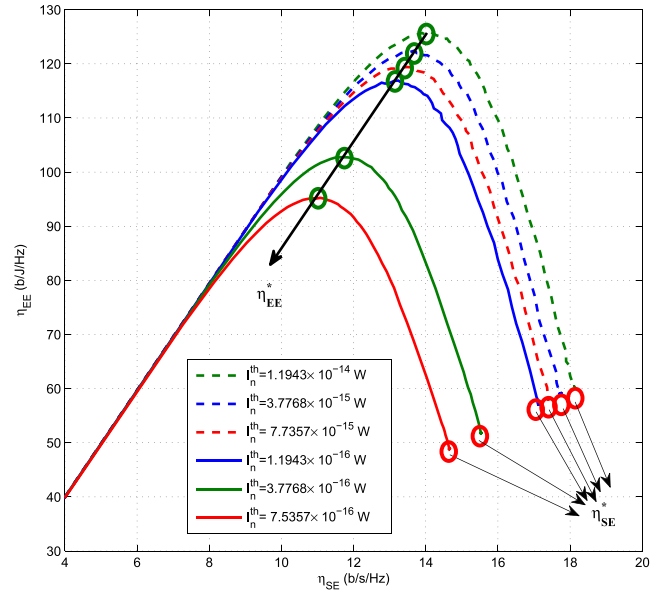


**FIGURE 6.**  $\eta_{EE}$  versus  $\eta_{SE}$  for various threshold interference levels  $I_n^{th}$ .

values of  $P^{\max}$ , the achievable  $\bar{\eta}$  decreases with  $P^{\max}$ . This is an important observation which can allow the flexibility to save more power by choosing the sensible  $P^{\max}$  which results in improving the achieved EE and SE.

Fig. 6 shows the EE-SE tradeoff of a macrocell overlaid with 4 pico BSs when  $P^{\max} = 0.2W$ , for the threshold interference level  $I_n^{th} = 1.1943 \times 10^{-14} W$ ,  $3.7768 \times 10^{-15} W$ ,  $7.7357 \times 10^{-15} W$ ,  $1.1943 \times 10^{-16} W$ ,  $3.7768 \times 10^{-16} W$  and  $7.7357 \times 10^{-16} W$ . The simulation results show that the maximum achievable EE and SE decreases monotonically

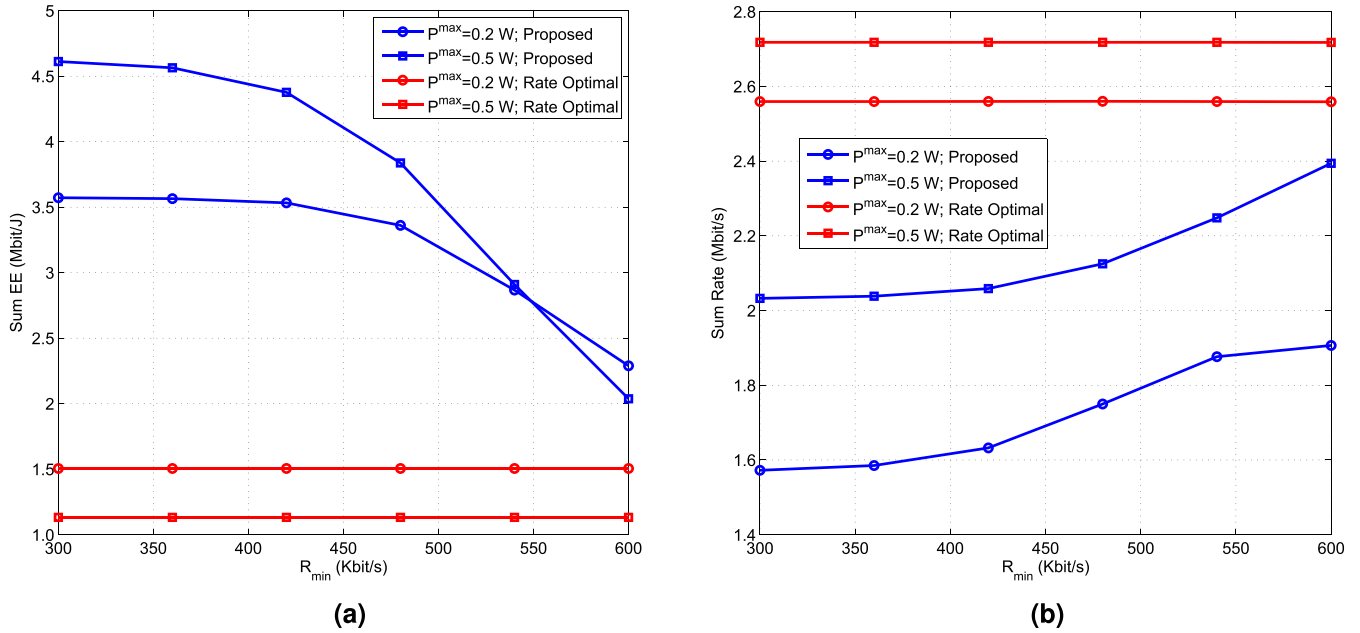


FIGURE 7. Sum EE and Sum Rate versus  $R_{min}$  for various values of  $P^{max}$ ,  $N = 4$ ,  $K = 4$ ,  $P_C = 0.1$  W and  $I_n^{th} = 1.1943 \times 10^{-14}$  W. (a) Sum EE versus  $R_{min}$ . (b) Sum rate versus  $R_{min}$ .

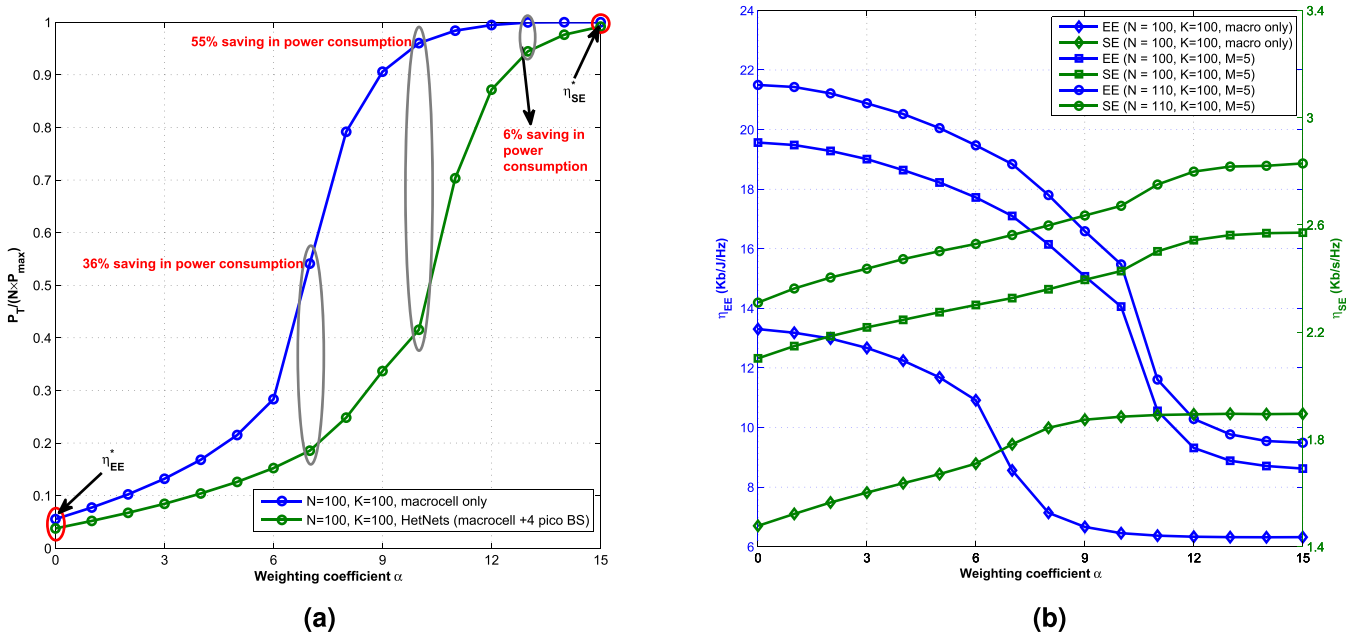


FIGURE 8. Relative Optimal transmit power,  $\eta_{EE}$  and  $\eta_{SE}$  versus weighted coefficient  $\alpha$  with  $N_{macro} = 0.2 * N$ ,  $N_0 = -174$  dbm/Hz and  $R_n^{min} = 4$  b/s/Hz. (a)  $\left(\frac{P_T}{N * P^{max}}\right)$  vs.  $\alpha$  for varying  $M$ . (b)  $\eta_{EE}$  and  $\eta_{SE}$  vs  $\alpha$  for varying  $N$  and  $M$ .

with  $I_n^{th}$ . The figure further reveals that the lower values of  $I_n^{th}$  results in higher achievable EE and SE in comparison to the lower achievable EE and SE at the higher values of  $I_n^{th}$ . We note that the maximum achievable EE is reduced from 126 b/J/Hz to 94 b/J/Hz when the  $I_n^{th}$  is reduced from  $1.1943 \times 10^{-14}$  W to  $7.7357 \times 10^{-16}$  W. Further, the figure shows that higher threshold interference level  $I_n^{th}$  achieves higher achievable EE and SE. For the remainder of the simulation results, we assume  $I_n^{th} = 1.1943 \times 10^{-14}$  W.

We present a baseline algorithm, namely, a rate-optimal algorithm which maximises the overall system rate. Figs. 7(a) and 7(b), which respectively shows the performance in terms of the sum EE and the sum rate versus  $R_{min}$ . We assume four users are randomly located within the coverage area. The two figures show that the proposed algorithm achieves a higher sum EE than the rate-optimal algorithm. The rate-optimal algorithm can achieve a higher sum rate, however, at a cost of reduction in EE. Moreover, both EE and

the sum rate increases with  $P^{\max}$ . It should be also noted that the sum EE decreases with  $R^{\min}$ , whereas the sum rate increases with it. We note that at  $R^{\min} = 600$  Kbit/s, the achievable EE at  $P^{\max} = 0.2$ W is higher than the achievable EE at  $P^{\max} = 0.5$ W. This is due to the fact that the normalisation factor  $\theta_{EE}$  depends on the maximum transmission power  $P^{\max}$ .

In order to measure the performance gains of two-tier HetNet configuration of  $M = 5$  as compared to a macrocell only  $M = 1$  with minimum rate requirement of 4 b/s/Hz, Fig. 8(a) and 8(b) show the plots for optimal average transmit power normalised by  $P^{\max}$  and achievable EE along with achievable SE versus weighted coefficient  $\alpha$  for varying number of users  $N$  resulting in user densities of 200 and 220 active UE's per  $\text{km}^2$  and  $K = 100$ . For the case of  $M = 1$ , all the users are served by macrocell  $N_{\text{macro}} = N$  whereas for  $M = 5$ , the number of users per macrocell are  $N_{\text{macro}} = 0.2 * N$  and number of users per pico BSs are  $N_{\text{small}} = N/M$ . It can be seen that the optimal transmit power  $P_{\eta}^*$  irrespective of  $M = 1$  and  $M = 5$  configurations monotonically increases with  $\alpha$ . It is worth to mention that power saving ( $P^{\max} - P_{\eta}^*$ ) of  $M = 5$  (denoted by green line) in comparison to  $M = 1$  (denoted by blue line) first monotonically increases with  $\alpha$  and afterwards it start decreasing as  $\alpha$  approaches towards  $\alpha_{EE}$ . Fig. 8(b) shows the corresponding achievable EE and SE in  $M = 1$  and  $M = 5$  at the optimal tradeoff transmit values ( $P_{\eta}^*$  as previously shown in Fig. 8(a)) versus  $\alpha$  for varying user densities and  $K = 100$ . Another observation is that achievable EE and SE also increases with an increase in number of user  $N$ . The figure reveals that for a given  $N$ ,  $K$  and  $\alpha$ , the two-tier HetNet configuration always outperforms in terms of both the power consumption and the achievable EE along with corresponding

achievable SE as compared to the traditional macrocell only configuration: by averaging over all the values of  $\alpha$ , the average achievable EE is 15.025 kb/J/Hz with average achievable SE of 2.358 kb/s/Hz and power consumption of 78.27 mW in  $M = 5$  for  $N = 100$  and  $K = 100$  compared to the average achievable EE of 9.216 kb/J/Hz with average achievable SE of 1.7525 kb/s/Hz and power consumption of 1842.236 mW in  $M = 1$  for  $N = 100$  and  $K = 100$ .

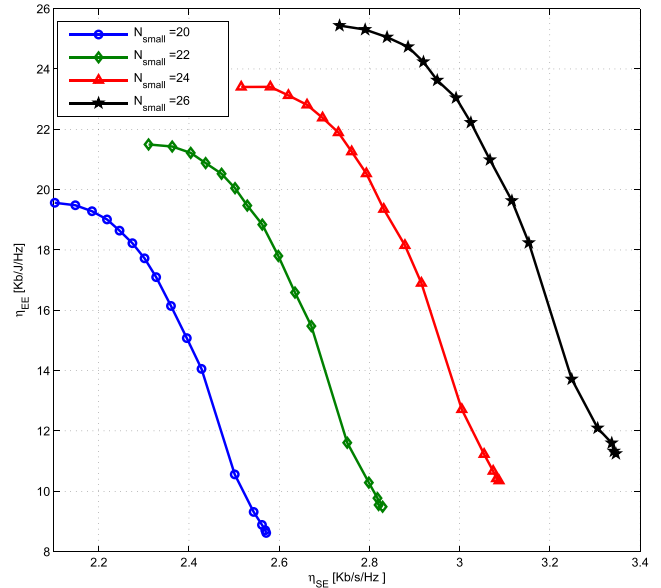


FIGURE 9.  $\eta_{EE}$  and  $\eta_{SE}$  of two-tier HetNet configuration for various values of  $N_{\text{small}}$  with  $K = 100$ ,  $M = 5$ ,  $N_0 = -174$  dbm/Hz and  $R_n^{\min} = 4$  b/s/Hz.

Fig. 9 shows the impact of the varying number of users per pico BS denoted by  $N_{\text{small}}$  on the EE-SE tradeoff in two-tier HetNets with 4 pico BSs lying on the cell edge of a macrocell.

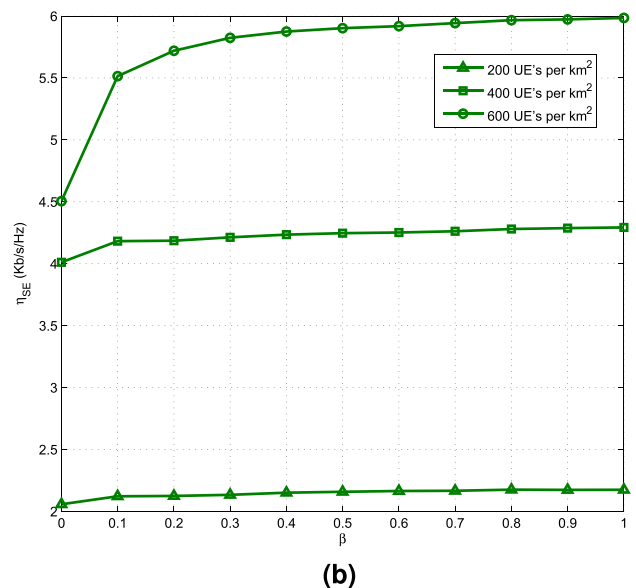
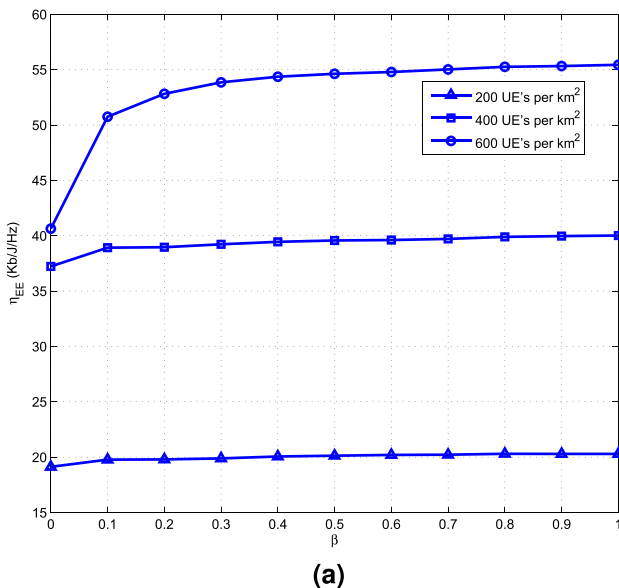


FIGURE 10.  $\eta_{EE}$  and  $\eta_{SE}$  versus  $\beta$  for varying user densities,  $P^{\max} = 0.2$ W,  $P_C = 0.1$ W and  $I_n^{th} = 1.1943 \times 10^{-14}$  W. (a)  $\eta_{EE}$  versus  $\beta$ . (b)  $\eta_{SE}$  versus  $\beta$ .

The total number of users per pico BS denoted by  $N_{\text{small}}$  are set to vary at 20, 22, 24 and 26. It is observed that when  $N_{\text{small}}$  is increased from 20 to 26, the EE-SE tradeoff curve expands which improves the achievable EE from 19.56 Kb/J/Hz to 25.44 Kb/J/Hz at  $\alpha = 0$  whereas the achievable SE improves from 2.102 Kb/s/Hz to 2.734 Kb/s/Hz due to multi-user diversity. For the given  $N_{\text{small}} = 20$  and  $\alpha = 3$ , the figure reveals the significant improvements in achievable EE (50% gain) and SE (39% gain) along with reduction in power consumption (47.5%) in case of two-tier HetNets as compared to the macrocell only configuration.

Fig. 10 shows the achievable EE and SE versus  $\beta$ , as defined in (1), ranging from 0 (macrocell only) to 1 increasing the number of pico BSs deployed on the edge of a macrocell from 1 to 40 with user densities set at 200, 400 and 600 active UE's per km<sup>2</sup> randomly deployed within the area of 500 × 500 m<sup>2</sup> and minimum rate requirement set as 4 b/s/Hz. It is evident from this figure that deploying pico BSs on the edge of a macrocell can achieve significant gains for all the performance metrics to satisfy the objectives and requirements of 5G systems. As it can be seen from the figure, the achievable EE and SE increase both with an increase in network densification and user density. The Het-Net configuration with  $\beta = 0.1$  which results in 4 pico BSs deployed on the cell edge of a macrocell with user density of 600 active UE's per km<sup>2</sup> achieves an area energy efficiency of 64.617 kb/J/Hz/km<sup>2</sup> as compared to 51.745 kb/J/Hz/km<sup>2</sup> for macrocell only, i.e.,  $\beta = 0$ . Similarly, an area spectrum efficiency at  $\beta = 0.1$  increases from 2.702 kb/s/Hz/km<sup>2</sup> to 5.325 kb/s/Hz/km<sup>2</sup> as user density is increased from 200 to 400 active UE's per km<sup>2</sup>. It is important to mention that introducing too many pico BSs can cause increase in the deployment and maintenance costs, backhauling costs and system complexity which are not considered in this analysis. However, it is evident from Fig. 10(a) and 10(b) that the tradeoff exists between deployed number of pico BSs and the achieved values of performance metrics subject to the given user density. For example, it is suitable to choose an optimal  $\beta$  as 0.2, 0.5 and 0.8 for the given user densities of 200, 400 and 600 active UE's per km<sup>2</sup> and afterwards, an increase in  $\beta$  result in a very minor improvement in performance metrics.

## VI. CONCLUSIONS

In this paper, the problem of simultaneously maximising the overall system EE and SE in an uplink of a two-tier OFDMA-based HetNet using adaptive channel and power allocation was addressed by considering the maximum transmission power, cross-tier interference threshold and users' minimum-QoS constraints. The quasi-concavity of the proposed approach was proved, and due to this property, the Pareto optimal solution was derived using LDD approach based on joint user association, subcarrier and power allocation. An iterative two-layer framework was proposed in which the outer layer was solved by Dinkelbach method as shown in Algorithm-1; whereas the inner layer was solved using

LDD approach as shown in Algorithm-2. From simulation results, we can refer two main observations. Firstly, SE is maximised at different values of weighted coefficient  $\alpha$  depending on the maximum transmission power. Secondly, our proposed tradeoff metric  $\alpha$  can help us to save much power by lowering the maximum transmission power. The tradeoff parameter  $\eta$  is an increasing function of transmission power for smaller values of  $P^{\text{max}}$ , whereas it is a decreasing function of transmission power for higher values of  $P^{\text{max}}$ .

## APPENDIX A PROOF OF LEMMA 1

In this Appendix, we prove that  $\eta$  is quasi-concave in  $\tilde{\sigma}_{k,n}^{(m)}$  and  $p_{k,n}^{(m)}$ .

$$\begin{aligned} \eta &= \frac{R}{P} \left( 1 + \alpha \frac{\theta_{\text{SE}} \times \eta_{\text{SE}}}{\theta_{\text{EE}} \times \eta_{\text{EE}}} \right) \\ &= \frac{R}{P} \left( 1 + \alpha \frac{\theta_{\text{SE}} \times P}{\theta_{\text{EE}} \times B} \right) \\ &= \frac{R}{P} (1 + \bar{\alpha}P) \\ &= \frac{R}{P} + \bar{\alpha}R = \eta_{\text{EE}} + \bar{\alpha}R \end{aligned} \quad (35)$$

where

$$\bar{\alpha} = \alpha \frac{\theta_{\text{SE}}}{\theta_{\text{EE}}B}$$

First, we prove that  $r_{k,n}^{(m)}$  is concave with respect to  $\tilde{\sigma}_{k,n}^{(m)}$  and  $p_{k,n}^{(m)}$ . By taking the first order derivative of  $r_{k,n}^{(m)}$  with respect to  $p_{k,n}^{(m)}$  we get

$$\frac{\partial r_{k,n}^{(m)}}{\partial p_{k,n}^{(m)}} = \max_{k \in \mathcal{K}_m, n \in \mathcal{N}} \frac{B_k \gamma_{k,n}^{(m)}}{\ln(2) \left( 1 + \gamma_{k,n}^{(m)} p_{k,n}^{(m)} \right)} \quad (36)$$

From (36), it is clear that  $\frac{B_k \gamma_{k,n}^{(m)}}{\ln(2) \left( 1 + \gamma_{k,n}^{(m)} p_{k,n}^{(m)} \right)}$  is strictly monotonically decreasing with  $p_{k,n}^{(m)}$  and thus  $\frac{\partial^2 r_{k,n}^{(m)}}{\partial p_{k,n}^{(m)2}} < 0$ . Since  $R$  is the linear combination or sum of  $r_{k,n}^{(m)}$ , and therefore,  $R$  is also concave in  $p_{k,n}^{(m)}$ . Using the same principle, we can also show that  $R$  is concave in  $\tilde{\sigma}_{k,n}^{(m)}$ .

Denote the superlevel sets of  $\eta_{\text{EE}}$  in order to prove the quasi-concavity as follow:

$$\tau_{\alpha} = \{ \tilde{\sigma}_{k,n}^{(m)} \geq 0, p_{k,n}^{(m)} \geq P_n^{\text{min}}, \forall k, m, n \mid \eta_{\text{EE}} \geq \alpha \}$$

$\eta_{\text{EE}}$  is quasi-concave in  $\tilde{\sigma}_{k,n}^{(m)}$  and  $p_{k,n}^{(m)}$ , if  $\tau_y$  is convex for any real number  $y$  [36]. When  $y < 0$ , no points exist on the contour  $\eta_{\text{EE}} = y$ . When  $y \geq 0$ ,

$\tau_y$  is equivalent to  $y \left( N \times P_C + \sum_{m \in \mathcal{M}} \sum_{k \in \mathcal{K}_m} \sum_{n \in \mathcal{N}} \tilde{\sigma}_{k,n}^{(m)} p_{k,n}^{(m)} \right) - \sum_{m \in \mathcal{M}} \sum_{k \in \mathcal{K}_m} \sum_{n \in \mathcal{N}} \tilde{\sigma}_{m,n}^{(k)} B_k \log_2 \left( 1 + \frac{\gamma_{k,n}^{(m)} p_{k,n}^{(m)}}{\rho_{(m)}^2 P_{L_n}^{(m)}} \right)$  which is convex. Hence,  $\eta_{\text{EE}}$  is quasi-concave in  $\tilde{\sigma}_{k,n}^{(m)}$  and  $p_{k,n}^{(m)}$ . Since  $R$  is

strictly concave in  $\tilde{\sigma}_{k,n}^{(m)}$  and  $p_{k,n}^{(m)}$ . Therefore,  $\eta$  is also quasi-concave in  $\tilde{\sigma}_{k,n}^{(m)}$  and  $p_{k,n}^{(m)}$ . Since  $P_T$  is monotonically increasing linear function of  $p_{k,n}^{(m)}$ , then  $\eta$  is also quasi-concave in  $P_T$ .

## APPENDIX B PROOF OF LEMMA II

Let us assume  $\eta^* = \max_{\tilde{\sigma}_{k,n}^{(m)}, p_{k,n}^{(m)}} \eta$  is an optimal solution to the objective function (17). Similar to [37],  $\mathcal{G}(\eta)$  can be equivalently written as:

$$\mathcal{G}(\eta) = \max_{\tilde{\sigma}_{k,n}^{(m)}, p_{k,n}^{(m)}} (\tilde{\eta} - \eta) \times \left( N \times P_C + \epsilon_0 \sum_{m \in \mathcal{M}} \sum_{k \in \mathcal{K}_m} \sum_{n \in \mathcal{N}} \tilde{\sigma}_{k,n}^{(m)} p_{k,n}^{(m)} \right)$$

If  $\eta = \eta^*$ , then  $\tilde{\eta} - \eta = \tilde{\eta} - \eta^* \leq 0$  which means  $\mathcal{G}(\eta^*) \leq 0$ . However, we can always find some  $\tilde{\sigma}_{k,n}^{(m)}$  and  $p_{k,n}^{(m)}$  that can make  $\tilde{\eta} = \eta^*$  which result in  $\mathcal{G}(\eta^*) = 0$ . Hence,  $\mathcal{G}(\eta) > 0$  if  $\eta < \eta^*$  and  $\mathcal{G}(\eta) < 0$  if  $\eta > \eta^*$ . Hence, it is proven that  $\mathcal{G}(\eta) = 0$  iff  $\eta = \eta^*$ .

## REFERENCES

- [1] D. Lopez-Perez, I. Guvenc, G. de la Roche, M. Kountouris, T. Q. S. Quek, and J. Zhang, "Enhanced intercell interference coordination challenges in heterogeneous networks," *IEEE Wireless Commun.*, vol. 18, no. 3, pp. 22–30, Jun. 2011.
- [2] Q. Ye, B. Rong, Y. Chen, M. Al-Shalash, C. Caramanis, and J. G. Andrews, "User association for load balancing in heterogeneous cellular networks," *IEEE Trans. Wireless Commun.*, vol. 12, no. 6, pp. 2706–2716, Jun. 2013.
- [3] Y. Dong, M. Sheng, S. Zhang, and C. Yang, "Coalition based interference mitigation in femtocell networks with multi-resource allocation," in *Proc. IEEE ICC*, Sydney, NSW, Australia, Jun. 2014, pp. 2695–2700.
- [4] K. Kikuchi and H. Otsuka, "Proposal of adaptive control CRE in heterogeneous networks," in *Proc. IEEE PIMRC*, Sydney, NSW, Australia, Sep. 2012, pp. 910–914.
- [5] C. S. Chen, F. Baccelli, and L. Roullet, "Joint optimization of radio resources in small and macro cell networks," in *Proc. IEEE VTC Spring*, Budapest, Hungary, May 2011, pp. 1–5.
- [6] C. C. Zarakovitis and Q. Ni, "Maximising energy efficiency in multi-user multi-carrier broadband wireless systems: Convex relaxation and global optimisation techniques," *IEEE Trans. Veh. Technol.*, doi: 10.1109/TVT.2015.2455536.
- [7] X. Ge, B. Yang, J. Ye, G. Mao, C.-X. Wang, and T. Han, "Spatial spectrum and energy efficiency of random cellular networks," *IEEE Trans. Commun.*, vol. 63, no. 3, pp. 1019–1030, Mar. 2015.
- [8] H. Pervaiz, L. Musavian, and Q. Ni, "Joint user association and energy-efficient resource allocation with minimum-rate constraints in two-tier HetNets," in *Proc. IEEE PIMRC*, London, U.K., Sep. 2013, pp. 1634–1639.
- [9] G. Miao, N. Himayat, Y. Li, and D. Bormann, "Energy efficient design in wireless OFDMA," in *Proc. IEEE ICC*, Beijing, China, May 2008, pp. 3307–3312.
- [10] G. Miao, N. Himayat, and Y. Li, "Energy-efficient transmission in frequency-selective channels," in *Proc. IEEE GLOBECOM*, New Orleans, LA, USA, Nov./Dec. 2008, pp. 1–5.
- [11] G. Miao, N. Himayat, G. Y. Li, and S. Talwar, "Low-complexity energy-efficient scheduling for uplink OFDMA," *IEEE Trans. Commun.*, vol. 60, no. 1, pp. 112–120, Jan. 2012.
- [12] F. Haider, C.-X. Wang, H. Haas, E. Hepsaydir, and X. Ge, "Energy-efficient subcarrier-and-bit allocation in multi-user OFDMA systems," in *Proc. IEEE VTC Spring*, Yokohama, Japan, May 2012, pp. 1–5.
- [13] L. Musavian and Q. Ni, "Effective capacity maximization with statistical delay and effective energy efficiency requirements," *IEEE Trans. Wireless Commun.*, vol. 14, no. 7, pp. 3824–3835, Jul. 2015.
- [14] C. C. Zarakovitis and Q. Ni, "Energy efficient designs for communication systems: Resolutions on inverse resource allocation principles," *IEEE Commun. Lett.*, vol. 17, no. 12, pp. 2264–2267, Dec. 2013.
- [15] S. Khakurel, L. Musavian, and T. Le-Ngoc, "Trade-off between spectral and energy efficiencies in a fading communication link," in *Proc. IEEE VTC Spring*, Dresden, Germany, Jun. 2013, pp. 1–5.
- [16] L. Deng, Y. Rui, P. Cheng, J. Zhang, Q. T. Zhang, and M. Li, "A unified energy efficiency and spectral efficiency tradeoff metric in wireless networks," *IEEE Commun. Lett.*, vol. 17, no. 1, pp. 55–58, Jan. 2013.
- [17] J. Tang, D. K. C. So, E. Alsusa, and K. A. Hamdi, "Resource efficiency: A new paradigm on energy efficiency and spectral efficiency tradeoff," *IEEE Trans. Wireless Commun.*, vol. 13, no. 8, pp. 4656–4669, Aug. 2014.
- [18] C. Xiong, G. Y. Li, S. Zhang, Y. Chen, and S. Xu, "Energy- and spectral-efficiency tradeoff in downlink OFDMA networks," *IEEE Trans. Wireless Commun.*, vol. 10, no. 11, pp. 3874–3886, Nov. 2011.
- [19] L. Xu, G. Yu, and Y. Jiang, "Energy-efficient resource allocation in single-cell OFDMA systems: Multi-objective approach," *IEEE Trans. Wireless Commun.*, doi: 10.1109/TWC.2015.2443104.
- [20] X. Ge et al., "Spectrum and energy efficiency evaluation of two-tier femtocell networks with partially open channels," *IEEE Trans. Veh. Technol.*, vol. 63, no. 3, pp. 1306–1319, Mar. 2014.
- [21] G. Bacci, E. V. Belmega, P. Meritopoulos, and L. Sanguinetti, "Energy-aware competitive power allocation for heterogeneous networks under QoS constraints," *IEEE Trans. Wireless Commun.*, vol. 14, no. 9, pp. 4728–4742, Sep. 2015.
- [22] G. Yu, Y. Jiang, L. Xu, and G. Y. Li, "Multi-objective energy-efficient resource allocation for multi-RAT heterogeneous networks," *IEEE J. Sel. Areas Commun.*, vol. 33, no. 10, pp. 2118–2127, Oct. 2015.
- [23] G. Lim, C. Xiong, L. J. Cimini, and G. Y. Li, "Energy-efficient resource allocation for OFDMA-based multi-RAT networks," *IEEE Trans. Wireless Commun.*, vol. 13, no. 5, pp. 2696–2705, May 2014.
- [24] J. Tang, D. K. C. So, E. Alsusa, K. A. Hamdi, and A. Shojaeifard, "Resource allocation for energy efficiency optimization in heterogeneous networks," *IEEE J. Sel. Areas Commun.*, vol. 33, no. 10, pp. 2104–2117, Oct. 2015.
- [25] H. Zhang, C. Jiang, N. C. Beaulieu, X. Chu, X. Wang, and T. Q. S. Quek, "Resource allocation for cognitive small cell networks: A cooperative bargaining game theoretic approach," *IEEE Trans. Wireless Commun.*, vol. 14, no. 6, pp. 3481–3493, Jun. 2015.
- [26] O. Galinina, S. Andreev, A. Turlikov, and Y. Koucheryavy, "Optimizing energy efficiency of a multi-radio mobile device in heterogeneous beyond-4G networks," *Perform. Eval.*, vol. 78, pp. 18–41, Aug. 2014. [Online]. Available: <http://www.sciencedirect.com/science/article/pii/S016653161400056X>
- [27] M. Ismail, A. T. Gamage, W. Zhuang, and X. S. Shen, "Energy efficient uplink resource allocation in a heterogeneous wireless medium," in *Proc. IEEE ICC*, Sydney, NSW, Australia, Jun. 2014, pp. 5275–5280.
- [28] L. P. Qian, C. Qian, Y. Wu, and Q. Chen, "Power controlled system revenue maximization in large-scale heterogeneous cellular networks," in *Proc. IEEE ICC*, Sydney, NSW, Australia, Jun. 2014, pp. 5269–5274.
- [29] S. Samarakoon, M. Bennis, W. Saad, and M. Latva-Aho, "Opportunistic sleep mode strategies in wireless small cell networks," in *Proc. IEEE ICC*, Sydney, NSW, Australia, Jun. 2014, pp. 2707–2712.
- [30] F. Pantisano, M. Bennis, W. Saad, and M. Debbah, "Spectrum leasing as an incentive towards uplink macrocell and femtocell cooperation," *IEEE J. Sel. Areas Commun.*, vol. 30, no. 3, pp. 617–630, Apr. 2012.
- [31] M. Z. Shakir, K. A. Qaraqe, H. Tabassum, M.-S. Alouini, E. Serpedin, and M. A. Imran, "Green heterogeneous small-cell networks: Toward reducing the CO<sub>2</sub> emissions of mobile communications industry using uplink power adaptation," *IEEE Commun. Mag.*, vol. 51, no. 6, pp. 52–61, Jun. 2013.
- [32] A. Abdelnasser, E. Hossain, and D. I. Kim, "Tier-aware resource allocation in OFDMA macrocell-small cell networks," *IEEE Trans. Commun.*, vol. 63, no. 3, pp. 695–710, Mar. 2015.
- [33] K. Son, S. Lee, Y. Yi, and S. Chong, "REFIM: A practical interference management in heterogeneous wireless access networks," *IEEE J. Sel. Areas Commun.*, vol. 29, no. 6, pp. 1260–1272, Jun. 2011.
- [34] M. Emmerich and A. Deutz, "Multicriteria optimization and decision making," Dept. Leiden Inst. Adv. Comput. Sci., Leiden Univ., Leiden, The Netherlands, Tech. Rep., 2006.
- [35] R. T. Marler and J. S. Arora, "Survey of multi-objective optimization methods for engineering," *Struct. Multidisciplinary Optim.*, vol. 26, no. 6, pp. 369–395, Apr. 2004.

- [36] S. Boyd and L. Vandenberghe, *Convex Optimization*. Cambridge, U.K.: Cambridge Univ. Press, 2004.
- [37] D. W. K. Ng, E. S. Lo, and R. Schober, "Energy-efficient resource allocation in OFDMA systems with large numbers of base station antennas," *IEEE Trans. Wireless Commun.*, vol. 11, no. 9, pp. 3292–3304, Sep. 2012.
- [38] W. Dinkelbach, "On nonlinear fractional programming," *Manage. Sci.*, vol. 13, no. 7, pp. 492–498, Mar. 1967. [Online]. Available: <http://www.jstor.org/stable/2627691>
- [39] W. Yu and R. Lui, "Dual methods for nonconvex spectrum optimization of multicarrier systems," *IEEE Trans. Commun.*, vol. 54, no. 7, pp. 1310–1322, Jul. 2006.
- [40] K. Seong, M. Mohseni, and J. M. Cioffi, "Optimal resource allocation for OFDMA downlink systems," in *Proc. IEEE Int. Symp. Inf. Theory*, Seattle, WA, USA, Jul. 2006, pp. 1394–1398.
- [41] E. Hossain, L. B. Le, and D. Niyato, *Radio Resource Management in Multi-Tier Cellular Wireless Networks*. New York, NY, USA: Wiley, 2013.
- [42] D. P. Palomar and M. Chiang, "A tutorial on decomposition methods for network utility maximization," *IEEE J. Sel. Areas Commun.*, vol. 24, no. 8, pp. 1439–1451, Aug. 2006.



**HARIS PERVAIZ** (S'10) received the M.Sc. degree in information security from the Royal Holloway University of London, in 2005, and the M.Phil. degree in electrical and electronic engineering from the Queen Mary University of London, in 2011. He is currently pursuing the Ph.D. degree with the School of Computing and Communication, Lancaster University, U.K. His main research interests are green heterogeneous wireless communications and networking,

5G and beyond, millimeter wave communication, and energy and spectral efficiency.

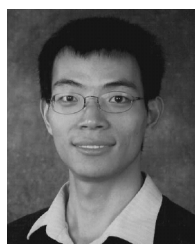


**LEILA MUSAVIAN** (S'05–M'07) received the Ph.D. degree in telecommunications from King's College London, U.K., in 2006. She was a Post-Doctoral Fellow with the National Institute of Scientific Research–Energy, Materials, and Telecommunications, University of Quebec, Canada, from 2006 to 2008. From 2009 to 2010, she was with Loughborough University and investigated adaptive transmission techniques for delay quality of service (QoS) provisioning in cognitive

radio networks (CRNs). From 2010 to 2012, she was a Research Associate with the Department of Electrical and Computer Engineering, McGill University, where she was involved in developing energy-efficient resource allocation techniques for multiuser wireless communications systems. She is currently a Lecturer in Communications with InfoLab21, School of Computing and Communications, Lancaster University. Her research interests lie in the area of wireless communications and include radio resource management for next generation wireless networks, CRNs, green communication and energy-efficient transmission techniques, and cross-layer design for delay QoS provisioning in spectrum-sharing channels.



**QIANG NI** (SM'08) received the B.Sc., M.Sc., and Ph.D. degrees from the Huazhong University of Science and Technology, China, all in engineering. He led the Intelligent Wireless Communication Networking Group with Brunel University London, U.K. He is currently a Professor and the Head of the Communication Systems Group with InfoLab21, School of Computing and Communications, Lancaster University, Lancaster, U.K. His main research interests lie in the area of wireless communications and networking, including green communications, cognitive radio systems, 5G, IoT, and vehicular networks. He was an IEEE 802.11 Wireless Standard Working Group Voting Member and a Contributor to the IEEE Wireless Standards.



**ZHIGUO DING** (S'03–M'05) received the B.Eng. degree in electrical engineering from the Beijing University of Posts and Telecommunications, in 2000, and the Ph.D. degree in electrical engineering from Imperial College London, in 2005. From 2005 to 2014, he was with Queen's University Belfast, Imperial College, and Newcastle University. Since 2014, he has been with Lancaster University as a Chair Professor. His research interests are 5G networks, game

theory, cooperative and energy harvesting networks, and statistical signal processing. He serves as an Editor of the IEEE TRANSACTIONS ON COMMUNICATIONS, the IEEE TRANSACTIONS ON VEHICULAR NETWORKS, the IEEE WIRELESS COMMUNICATION LETTERS, the IEEE COMMUNICATION LETTERS, and the *Journal of Wireless Communications and Mobile Computing*. He received the best paper award in the IET Communications Conference on Wireless, Mobile and Computing in 2009, the IEEE Communication Letter Exemplary Reviewer in 2012, and the EU Marie Curie Fellowship from 2012 to 2014.

• • •